2004

# Damage Modeling Method For Turbine Compressor Blade Tuning

Gennadiy Afanasiev
*University of Central Florida*

# DAMAGE MODELING METHOD FOR TURBINE COMPRESSOR BLADE TUNING

by

GENNADIY AFANASIEV
B.S. University of South Florida, 1996

A thesis submitted in partial fulfillment of the requirements
for the degree of Master of Science
in the Department of Mechanical, Materials and Aerospace Engineering
in the College of Engineering and Computer Science
at the University of Central Florida
Orlando, Florida

Spring Term
2004

# ABSTRACT

The thesis presents a method of evaluation for blade damage in Combustion Turbine Compressor Section. This method involves use of multiple domains within a single Finite Element Model to predict the effect of damage on the blade properties. This approach offers significant time and effort savings when compared to traditional evaluation methods of similar problems. It is demonstrated via examples that the "multi-domain" modeling approach yields acceptable accuracy results.

The economical implications of described method are readily applicable to both the industrial and the aerospace Combustion Turbine fields. It is economically impractical to replace the blade at each damage occurrence. However, the evaluation time involved in making associated decisions can be extensive if traditional methods of evaluation are used.

The specific contributions of this study are twofold:

1. Time savings during evaluation
2. Compressor Blades may be returned to service which are otherwise replaced

# TABLE OF CONTENTS

# LIST OF FIGURES

# LIST OF TABLES

# LIST OF ABBREVIATIONS

BPF ---------- Blade Passing Frequency

CF ---------- Centrifugal Force

DOF ---------- Degrees of Freedom

FEA ---------- Finite Element Analysis

FEM ---------- Finite Element Model

FO ---------- Forced Outage

GB ---------- Gas Bending

GT ---------- Gas Turbine

ID ---------- Identification (name)

LE ---------- Leading Edge

PO ---------- Planned Outage

RPM ---------- Revolutions per Minute

SB ---------- Service Bulletin

SF ---------- Safety Factor

SWPC ---------- Siemens Westinghouse Power Corporation

TE ---------- Trailing Edge

# CHAPTER ONE: INTRODUCTION

## Combustion Turbine Overview

Of the various means of producing mechanical power, the turbine is in many respects the most satisfactory. The absence of reciprocating and rubbing members means that balancing problems are few, that the lubricating oil consumption is exceptionally low, and that reliability can be high. The inherent advantages of the turbine were first realized using water as the working fluid, and hydro-electric power is still a significant contributor to the world's energy resources. Around the turn of the twentieth century, the steam turbine began its career and, quite apart from its wide use as a marine power plant, it has become the most important prime mover for electricity generation. Steam turbine plants producing over 500 MW of shaft power with an efficiency of nearly 40 percent are now being used. In spite of its successful development, the steam turbine does have an inherent disadvantage. It is that the production high pressure high temperature steam involves the installation of bulky and expensive steam generating equipment, whether it be a conventional boiler or a nuclear reactor. The significant feature is that the hot gases produced in the boiler furnace or reactor core never reach the turbine; they are merely used indirectly to produce an intermediate fluid, namely steam. Clearly a much more compact power plant results when the water to steam step is eliminated and the got gases themselves are used to drive the

turbine.

Serious development of the gas turbine began not long before the Second World War with shaft power in mind, but attention was soon transferred to the turbojet engine for aircraft propulsion. Gas turbines began to compete successfully in the other field only in the mid nineteen fifties, but since then it has made a progressively greater impact in an increasing variety of applications [1], [2].

In order to produce an expansion through a turbine, a pressure ratio must be provided, and the first necessary stop in the cycle of a gas turbine plant must therefore be compression of the working fluid. If after compression the working fluid were to be expanded directly in the turbine, and if there were no losses in either component, the power developed by the turbine would just equal that absorbed by the compressor. Thus if the two were coupled together, the combination would do no more than just rotate. But the power developed by the turbine can be increased by the addition of energy to raise the temperature of the working fluid prior to expansion. When the working fluid is air a very suitable means of doing this is by combustion of fuel in the air which has been compressed. Expansion of the hot working fluid then produces a greater power output from the turbine, so that it is able to provide a useful output in addition to the power necessary to drive the compressor. This represents the gas turbine or internal-combustion turbine in its simplest form. The three main component are a compressor, combustion chamber and turbine, connected together. The main concern of the present thesis is the Compressor section of the Combustion Turbine [1], [2], [3]. However, all main components are illustrated on the Figure 1.

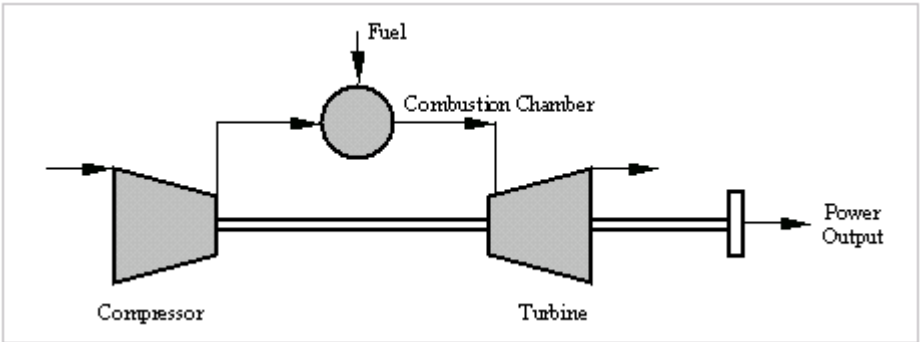


Figure 1. Simple Combustion Turbine Cycle.

The research study conducted within the scope of this thesis is focused on Siemens Westinghouse Combustion Turbines. Figure 2 below shows a 3-D cross-section of W501F engine of approximately 200 MW capacity.

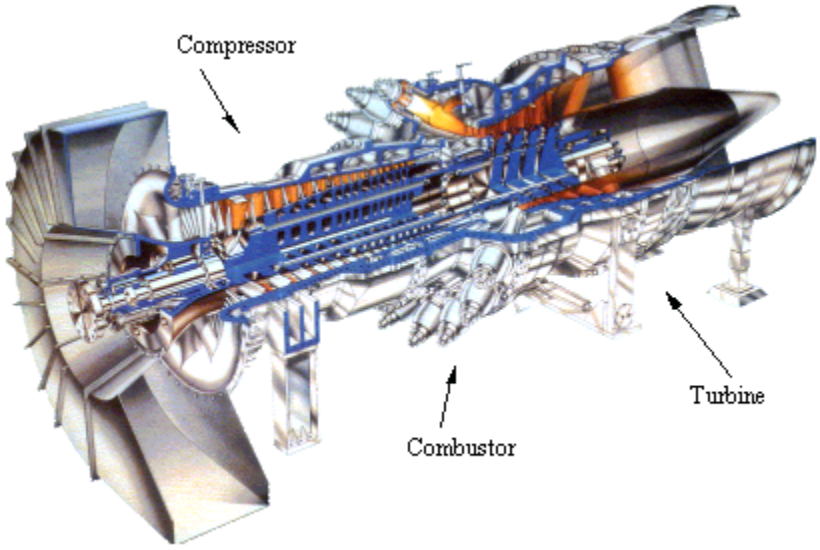


Figure 2. Siemens Westinghouse W501F Combustion Turbine.

## Compressor Overview

The combustion turbine receives air from the compressor and raises it to a high energy level by mixing in fuel and burning the mixture, after which products of the combustor are expanded through the turbine. The function of the Compressor is to serve as an air pump, converting low pressure, low density ambient air into a high pressure air prior to delivering it to the combustor. Of three primary working parts of the combustion turbine, the compressor is the first component acting on the incoming air at it flows through the inlet. Thus its design and behavior are particularly critical with any shortcomings likely to be reflected in reduced effectiveness of the downstream components since their operation is dependent on compressor output [1].

There are two types of compressors used on combustion turbines: axial and centrifugal. From an early stage in the history of the gas turbine, it was recognized that the axial flow compressor had the potential for both a higher pressure ratio and a higher efficiency than the centrifugal compressor. Another major advantage was the much larger flow rate for a given frontal area. These potential gains have now been fully realized as the result of intensive research into the aerodynamics of axial compressors: the axial flow machine dominates the field for large powers and the centrifugal compressor is restricted to the lower end of the power spectrum where the flow is too small to be handled efficiently by axial blading. Early axial flow units had pressure ratios of around 5:1 and required about 10 stages. Over the years the overall pressure ratios available have risen dramatically, and some turbofan engines have pressure ratios of around 30:1. The typical industrial combustion turbine of 150 MW power output has around 12:1 pressure ratio axial compressor.

Continued aerodynamic development has resulted in a steady increase in stage pressure ratio, with the result that the number of stages for a given overall pressure ration has been greatly reduced. There has been in consequence a reduction in engine weight for a specified level or performance, which is particularly important for aircraft engines. It should be noted, however, that high-stage pressure ratios imply high Mach numbers and large gas deflections in the blading which would not generally be justifiable in an industrial gas turbine where eight is not critical; industrial units built on a much more restricted budget than an aircraft engine, will inevitably use more conservative design techniques resulting in more stages [3]. Siemens Westinghouse industrial gas turbines are typically equipped with 16-19 stage compressor. The axial compressor consists of a series of stages, each stage comprising a row of rotor blades followed by a row of stator blades. The air is initially accelerated by the rotor blade, and then decelerated in the stator blade passages wherein the kinetic energy transferred in the rotor is converted to static pressure. The process is repeated in as many stages as are necessary to yield the required overall pressure ratio.

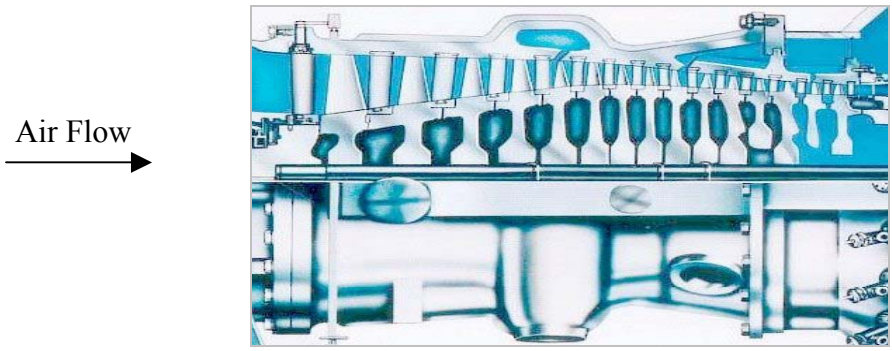


Figure 3. Siemens Westinghouse Axial Compressor, 15 stages.

## Thesis Topic Overview

Combustion Turbines are common in the modern world. Although the topic of Combustion Turbines is quite broad, the present thesis will concern specific issues. All included analyses and associated examples will concern Industrial Combustion Turbine. However, the proposed method is thought to be applicable to a general Combustion Turbine family.

Combustion Turbine Compressor blades are susceptible to damage. The cause of such damage typically involves foreign object ingestion. It can also be a result of mishandling of parts during transit or installation. Since compressor blades are subjected to high steady and oscillating loads during operation, it is critical to evaluate each impact / indication and take proper action to prevent blade failure as it could lead to severe downstream damage. The integrity of the blade is degraded since each damage / indication introduces a stress concentration. It is economically impractical to replace blades upon each damage incident. Instead, it is desired to develop a certain damage evaluation criteria [4].

Combustion Turbine Compressor blades are designed following certain criteria which dictate associated properties related aerodynamics and mechanical characteristics. This thesis will be specifically concerned with mechanical design and evaluation. This statement is given based on the fact that the associated damage being evaluated is considered insignificant from the aerodynamic standpoint. Furthermore, the conservative approach of damage allowance will ensure that the aerodynamic properties of the damaged blade are not degraded significantly [4].

The mechanical aspect of Compressor Blade design includes several basic disciplines. Namely: vibratory and steady loading, and vibratory response. It is critical to determine in every

case what effect on each of the listed properties a certain damage will have during operation. The typical approach available in industry consists of evaluating the damage per given criteria and determining the final disposition for a given blade. Among possible disposition choices are: replace, use as-is or blend. It is the main topic of the present thesis to demonstrate how the choice above is made and introduce a method for determining the final recommendation for blade service. Specifically it is proposed to apply the Finite Element Method to predict what effect the amount of damage at a particular location on the blade will have on two blade properties: vibratory and steady state response [4]. Furthermore, it is illustrated with examples how the proposed method is applied to a given Industrial Combustion Turbine Compressor Blade(s).

## Contribution

It is proposed and demonstrated in this thesis how a multi-domain Finite Element model can be used to evaluate the compressor blade damage. Namely the vibratory properties of the compressor blade are examined using a multi-domain finite element model. This method is given in comparison with traditional detailed model which assumes additional time and resources given the complexity of this issue [5]. It is demonstrated that, by simulating the damage on a given compressor blade by introducing the additional domain into the finite element model, it is possible to achieve acceptable accuracy results with significantly less computer time.

Typical blade damage in the Combustion Turbine Compressor is evaluated based on

photographs and measurements. In general the decision is made on whether on not the damage can be blended out to reduce the stress concentration near impact. This is done based on the fact that impact location typically contains sharp edges and uneven surface deflected regions. By physically removing these irregularities (blending) it is sometimes possible to return the blade into service with relatively small risk of failure. The diagram below (Figure 4) illustrates the example of a compressor blade blend vs. original damage.

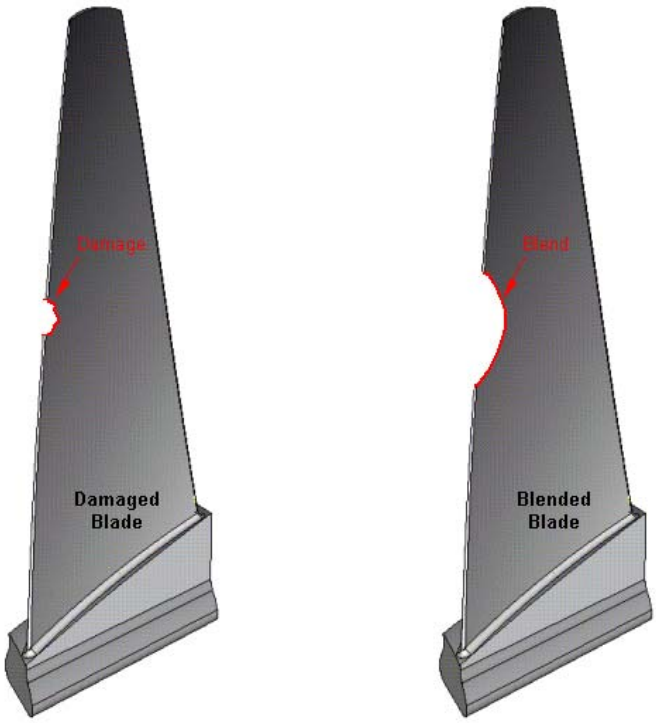


Figure 4. Damage vs. Blend on Blade.

Therefore, the dynamic properties of the blade will be different by some unknown amount. Furthermore, the specific change of dynamic characteristics of the blade will directly

depend upon the size and the location of a given blend. The important information required to make decisions for continued service of a given blade is whether or not the blade with blend still meets the original design criteria, and, if not, what is the risk of continue operation? These questions can be addressed either experimentally through strain gage testing or analytically through FE Analysis. The first method (testing) is typically impractical due to time required to conduct effective test(s) vs. time available for making the decision. So, this leaves us almost exclusively with analytical method.

As mentioned above in the Thesis Topic Section, analytical methods include detailed modeling of a given blend with subsequent analyses and comparing the results against design criteria and original (base) model. Essentially this means two sets of analyses: a base model analyses set and a blended model analyses set. Requirement of a second set comes from the fact that the proposed blend must be evaluated using the same exact boundary and loading conditions such that the differences due to blend can be detected. Please, note that the analysis work is doubled since the base model must be evaluated as well, all due to the fact that the alteration of the blade due to blend took place. This thesis document illustrates how the same information as typically extracted from two FE Models can be obtained from a single FE Model. The proposed multi-domain technique can make use of one model and simulate multiple scenarios with respect to blade blends. In fact, this especially convenient to conduct what-if studies to determine the most appropriate blend size, position and combination of blend along the leading and trailing edges of the blade.

How is this multi-domain technique setup? It is setup through applying various material properties to the blended areas vs. the rest of the blade. The main idea is to simulate the

difference in stiffness between the blended locations and the rest of the blade. In other words this is effective way to simulate the "absence" of metal where blend was performed. Chapter Three of this thesis contains details on what material properties are adjusted and how. However, in brief the mass density and the dynamic modulus (explained later) of elasticity are lowered. The diagram below (Figure 5) illustrates the basic concept behind the multi-domain model technique. Please, note that this diagram is an example only and does not correlate with the actual analysis performed in the Chapter Three of this Thesis.

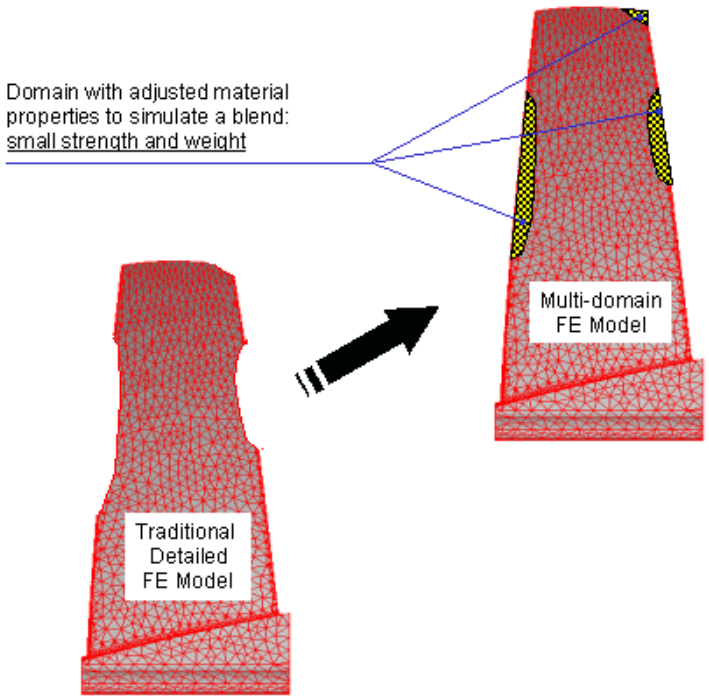


Figure 5. Multi-domain Technique Diagram (example only).

The advantage of the proposed technique is two-fold: significant time savings, and the

possibility of "what-if" studies of combination of different blends. While the traditional method requires a unique model for each blend in addition to the base model the single multi-domain model can be used for studying of several blends and blend combinations. Please, see the diagram below (Figure 6).

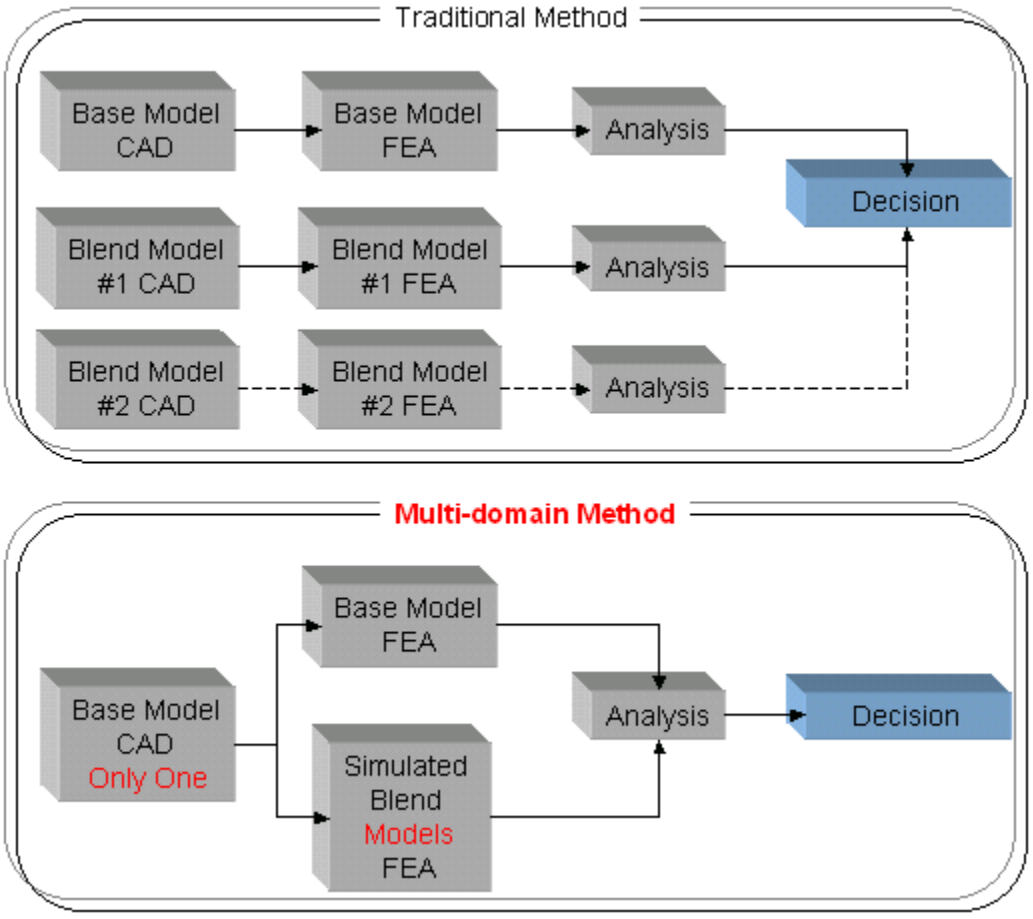


Figure 6. Analysis Process: traditional vs. multi-domain method.

# CHAPTER TWO: LITERATURE REVIEW

The Combustion Turbine industry is highly specialized and unique when it comes to service and damage considerations. It becomes even more specialized when this industry is split into aerospace and industrial combustion turbines. The research information is limited and mostly confidential to a specific firm or corporation [6]. The subject of service parts and risk associated with running compromised components is highly competitive. However, this does not preclude the author from investigation the subject of this thesis document and deriving conclusions. The lack of readily accessible information however, does affect the amount of literature reviewed required in this chapter of the thesis per UCS guidelines. Having stated that the following literature study has been conducted:

1. Existing (traditional) method for Compressor Blade Damage Evaluation
2. Combustion Turbine Compressor Blade Dynamic Design Criteria

Item 1 above sources of information include either the public (university) library system or company confidential reference documents. Item 2 sources are company confidential information only.

## Library Research

Item 1 above yielded no information through the university library system. This most likely is due to reasons stated in the beginning of this chapter. Typical information contents available through the library system are related to general design concepts. Also, due to harsh thermal and acoustic environment in the turbine section of the combustion turbine engine, most of the research material is focused on this "hot" section of the engine. The Figure 7 below illustrates typical findings when using the web-search system.

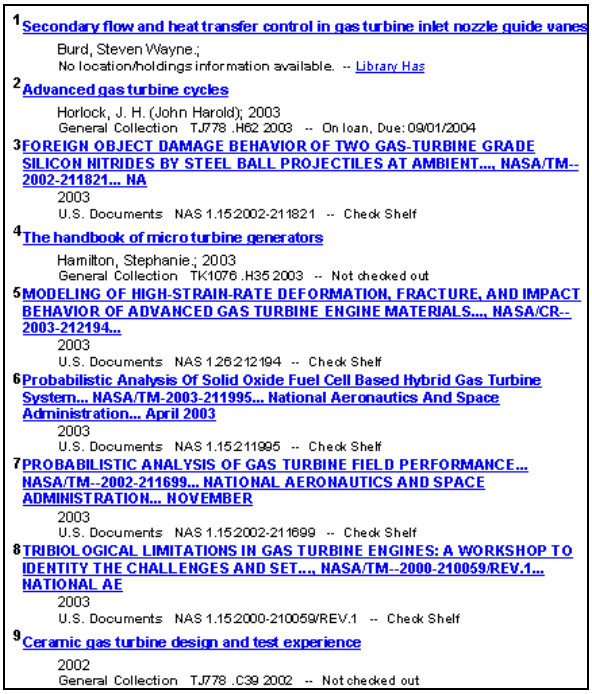
1 Secondary flow and heat transfer control in gas turbine inlet nozzle guide vanes
Burd, Steven Wayne.;
No location/holdings information available. -- Library Has
2 Advanced gas turbine cycles
Horlock, J. H. (John Harold); 2003
General Collection TJ778 .H62 2003 -- On loan, Due: 09/01/2004
3 FOREIGN OBJECT DAMAGE BEHAVIOR OF TWO GAS-TURBINE GRADE SILICON NITRIDES BY STEEL BALL PROJECTILES AT AMBIENT..., NASA/TM--2002-211821... NA
2003
U.S. Documents NAS 1.15:2002-211821 -- Check Shelf
4 The handbook of micro turbine generators
Hamilton, Stephanie.; 2003
General Collection TK1076 .H35 2003 -- Not checked out
5 MODELING OF HIGH-STRAIN-RATE DEFORMATION, FRACTURE, AND IMPACT BEHAVIOR OF ADVANCED GAS TURBINE ENGINE MATERIALS..., NASA/CR--2003-212194...
2003
U.S. Documents NAS 1.26:212194 -- Check Shelf
6 Probabilistic Analysis Of Solid Oxide Fuel Cell Based Hybrid Gas Turbine System... NASA/TM-2003-211995... National Aeronautics And Space Administration... April 2003
2003
U.S. Documents NAS 1.15:211995 -- Check Shelf
7 PROBABILISTIC ANALYSIS OF GAS TURBINE FIELD PERFORMANCE... NASA/TM--2002-211699... NATIONAL AERONAUTICS AND SPACE ADMINISTRATION... NOVEMBER
2003
U.S. Documents NAS 1.15:2002-211699 -- Check Shelf
8 TRIBIOLOGICAL LIMITATIONS IN GAS TURBINE ENGINES: A WORKSHOP TO IDENTITY THE CHALLENGES AND SET..., NASA/TM--2000-210059/REV.1... NATIONAL AE
2003
U.S. Documents NAS 1.15:2000-210059/REV.1 -- Check Shelf
9 Ceramic gas turbine design and test experience
2002
General Collection TJ778 .C39 2002 -- Not checked out

Figure 7. Typical library findings on Combustion Turbine.

Overall, it is was not possible to obtain library material directly related to the topic of this thesis due to its very specific nature: compressor blade damage evaluation. It is author's opinion that this subject is not currently covered in the public library system and most likely will not be covered in the future.

Regarding the company confidential reference information. The author explored the SWPC library for Compressor Blade damage technique and was able to find several relevant proprietary reports on this subject [4], [5], [7]. Although it is not possible to cite the reports in this thesis directly, general summary can be provided of topics covered and conclusions drawn. As with previous exercise surveying the public library system it was found that the majority of damage evaluation and methods were focused on the turbine section of the engine. One report however, was retrieved on the subject of the compressor blade damage [5]. It was developed to provide guideline for how much damage compressor blades and vanes can sustain based on their strength properties, and how a small damage could effect the local stress field near the damaged location. It is important to note that, although thorough, this report's intention was only to cover small damages (nicks and dents <= .030"). The mentioned report's conclusions contained general recommendations on whether or not a given damage must be blended vs. operating as-is. The allowable blend recommendations are outside of the report's scope.

At the same time many reports were obtained containing details of analysis of a given blend via the traditional method as described in Chapter One of this thesis document [3], [4], [6], [7]. This is a very important point because it confirms the author's statement in the contribution section regarding current techniques of damage evaluation. Specifically, the damage evaluation report typically contains damage information and the CAD Model details of the base model and

of the blended model, i.e. two models and analysis details. Figure 8 shows the model "tree" setup and a total of five CAD and FEA models were created to study blends of different size on this Combustion Turbine Compressor Vane.

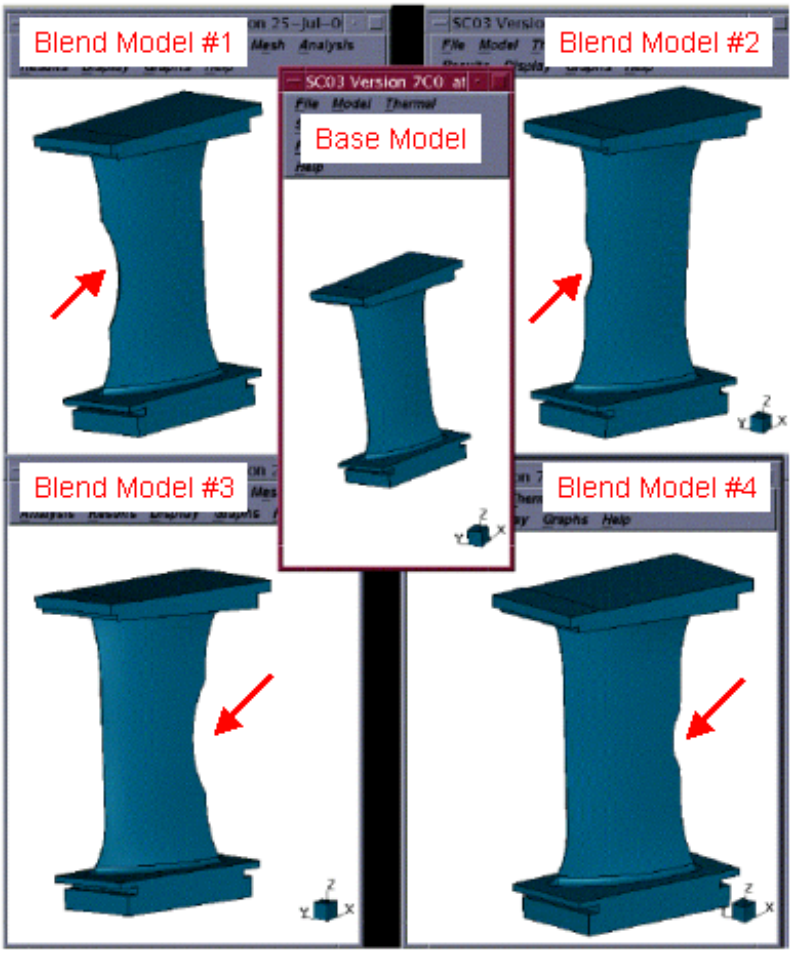


Figure 8. Typical Blend Study Model "Tree".

For the traditional evaluation method each blend variation required a unique CAD and FEA model as shown on Figure 8 above.

## Compressor Blade Dynamic Design Criteria and Blade Tuning

Dynamic considerations play an important role in the design of a number of combustion turbine components including compressor blades, particularly when rotational speeds are high. Dynamic analysis, in the past mostly aimed only to the computation of the critical speeds, but currently in many instances used to obtain a whole picture of the rotor-dynamic behavior of the machine (e.g., the computation of the Campbell diagram illustrated in the following paragraphs), must accompany stress analysis and all the other computations related to the working conditions of the machines (e.g. aero dynamic study) [8].

The specific focus of this study is given to the natural frequencies of the blade vs. know driver frequencies at rated engine speed. This study is commonly referred to as "blade tuning". The basic principle behind this study is to make sure that the blade natural frequencies are not coincident with the driving alternating forcing frequencies. Each stage blade in the turbine compressor is tuned separately because of the geometry, stiffness, weight and adjacent hardware differences. However, in each case the mathematical and graphical representation is similar and is presented using common convention for consistency and ease of interpretation.

Naturally the criteria associated with blade tuning are not the same for all combustions turbines. The criteria will vary with intended use, operating conditions, size and design philosophy. Because of the fact that the author of this thesis is currently employed by Siemens Westinghouse Power Corporation most design philosophy fundamentals will be of the said company [4]. For the discussion purposes this will be sufficient and it will only help to demonstrate the general technique.

The details of models comparison and how the design philosophy affects the conclusion is not entirely relevant to the matter of contribution which is clamed in this thesis. What is relevant is that the same philosophy is used consistently throughout this thesis and that recommendations for future use are made with appropriate remarks of being dependant on a given design criteria. In all cases the design criteria (philosophy) must be followed for a specific product as dictated by the associated manuals and/or standards.

As mentioned above, the graphical representation of the blade tuning process is consistent for all rows and all blade sizes. Campbell Diagrams are typically used to illustrate the dynamic properties of the blade vs. known system drivers for the rated equipment speed. The figure on the following page (Figure 9) illustrates the typical Campbell Diagram with associated terminology of each item. Per SPWC design criteria: Natural modal frequencies $\mathbf{f_i}$ at design speed $\mathbf{f_D}$ should be tuned to avoid resonance. The design speed depends on the frequency in the power lines for a given customer. For the duration of this thesis the 60Hz system will be assumed corresponding to 3600 RPM running (design) speed [4], [9], [10], [11].

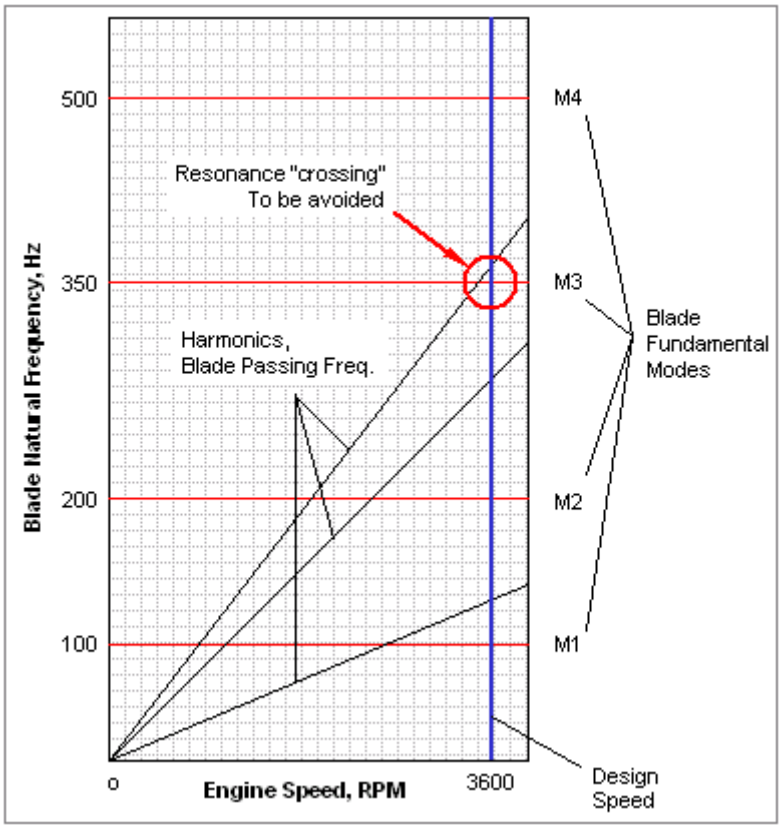


Figure 9. Typical Campbell Diagram.

The Figure above (Figure 9) illustrates the typical Campbell Diagram construction. This diagram is designed to provide graphical representation of the relationship between blade vibration modes and the anticipated forcing function frequencies.

Construction of the Campbell Diagram is one of the fundamental steps in the blade tuning process. This diagram and associated terminology will be referred to throughout this thesis [4], [12].

The horizontal (x) axis labeled “RPM” represents the engine running speed in revolutions

per minute. The vertical (y) axis represents the frequency, thus this diagram is a function of frequency vs. engine running speed. Horizontal red lines on the diagram (Figure 9) are the blade frequency modes determined by modal analysis. The number of these modes is set by given design criteria [4]. In all subsequent examples contained in Chapter Three, the number of modes will be six as per the current SWPC compressor blade design criteria. The diagonal lines initiating from the origin in the Campbell Diagram signify frequencies associated with all known vibratory drivers. Once again these are set by the blade design criteria. In the following analysis details (Chapter Three) these known drivers will consist of those prescribed by the SWPC design criteria. Examples of those include harmonics of rotation, upstream and downstream blade count in all cases multiplied by the engine speed:

$$H_1 = 1 * RPM$$

$$H_2 = 2 * RPM$$

where H1 and H2 are first and second harmonics of rotation. Or:

$$B_{up} = Z_{up} * RPM$$

where $B_{up}$ is the frequency due to the upstream blade / vane count and $Z_{up}$ is the upstream blade / vane count [4], [12].

The "crossing" region in the Figure 9 illustrates the case where one of the modes, Mode 3 (M3) in this case, involves a frequency coinciding closely with the known driver frequency. This kind of crossing must be avoided by changing the blade stiffness and/or weight. This process is iterative and it is called "Blade Tuning". The diagram and associated terminology above is provided in general terms.

Next, the specific blade tuning requirements as prescribed by SWPC blade design criteria

are provided so that the analysis effort described in the Chapter Three of this thesis is based on this specific blade tuning criteria. Refer to Figure 10, below according to [4].

| | **Excitation** | Tuning |
|---|---|---|
| General | (Distortion) | $f_1, f_2, f_3 \neq H \times f_R$ (H= 1,2,3,4,5,6) |
| | Inlet Strut, $Z_s$ (=8) | $f_1, f_2, f_3 \neq Z_s \times f_R$ (for rows 1 thru 4) |
| | Upstream Vane Number, $Z_{ups}$ | $f_1, f_2, f_3, f_4, f_5, f_6 \neq Z_{ups} \times f_R$ |
| | Downstream Vane Number, $Z_{dwn}$ | $f_1, f_2, f_3, f_4, f_5, f_6 \neq Z_{dwn} \times f_R$ |
| Special | Difference of Vane Number, $Z_{Di}$ | $f_1 \neq Z_{D1} \times f_R$, and $Z_{D2} \times f_R$ |
| | Electric Excitation, $f_e$ | $f_1 \neq f_e, 2f_e$ |
| | Bleed Slots, $Z_{SL}$ | $f_1, f_2, f_3 \neq Z_{SL}$ |

Note:

$f_i$ : Blade frequency for mode "i"

i = 1
i = 2
i = 3
i = 4
i = 5
i = 6

$f_R$ : Speed of rotation

H : Harmonics of rotation (Integer multiple number)

$Z_{ups}$ : Upstream Vane Number

$Z_{dwn}$ : Downstream Vane Number

$Z_D$ : Difference of Vane Number

$$\left(Z_{D1} = \left|Z_{dwn} - Z_{ups}\right|,\ Z_{D2} = \left|Z_{ups} - Z_{ups-1}\right|\right)$$

$Z_S$ : Inlet Strut Number

Figure 10. SWPC Blade Tuning Criteria.

In conjunction with the diagram shown on Figure 11 the blade tuning criteria is explained. The diagram below (Figure 11) is constructed to illustrate specific items from the blade tuning criteria. It is shown here with the assumption that the Row 1 compressor blade is being tuned. This is done so because the analysis demonstrated in Chapter Three is performed on Row 1 compressor blade as well. It is convenient, therefore, to consistently review the same blade throughout the thesis.

The downstream ($Z_{dwn}$) and the upstream ($Z_{ups}$) blade counts are calculated from the existing hardware of the downstream and the upstream compressor rows. In this case the downstream blade count is related to the Row 1 stationary airfoils (diaphragms) and the upstream blade count is related to the Inlet Guided Vanes (IGVs). The inlet strut count is related to the number of stationary structural members of the inlet cylinder, called struts. See Figure 11 below for details.

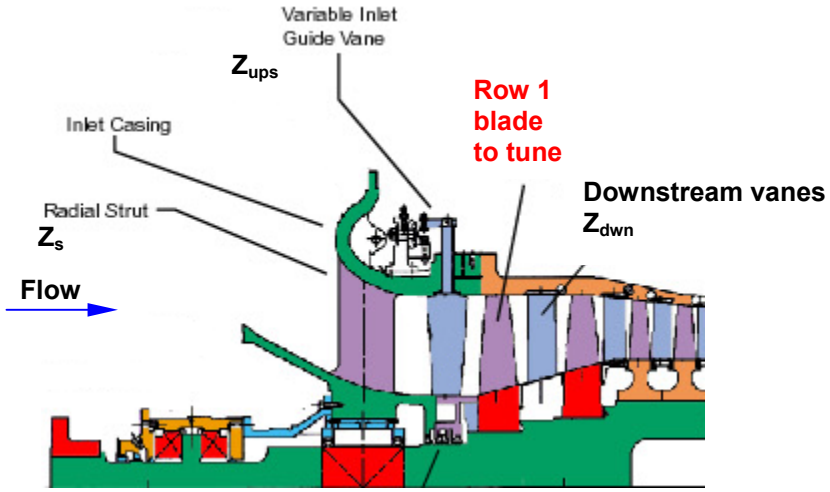


Figure 11. Vibratory Drivers Components.

The process of blade tuning is essential to mechanical blade design. Once the initial Campbell Diagram is constructed based on the particular blade design it is examined for "crossings".

The design criteria define the acceptable frequency bands for each mode. Furthermore, it is required that different ambient running conditions are evaluated due to the blade base metal dynamic modulus dependence on the temperature. Also, the manufacturing tolerance must be taken into consideration because the variations of blade physical dimensions affect the natural frequency values [4]. Since the thesis topics of interest is focused only on detecting the changes in vibratory properties of the blade, the analysis demonstrated in the Chapter Three will be limited to the ISO conditions and the nominal blade dimensional configuration. This is done to narrow the scope of the research and to focus only on the contribution as described in the beginning of this thesis.

The Dynamic Modulus is measured per the Test Method described in ASME E-1875. This test method measures the resonant frequencies of test specimens of suitable geometry by exciting them at continuously variable frequencies. Mechanical excitation of the bars is provided through the use of a transducer that transforms a cyclic electrical signal into a cyclic mechanical force on the specimen. A second transducer senses the resulting mechanical vibrations of the specimen and transforms them into an electrical signal. The amplitude and frequency of the signal are measured by an oscilloscope or other means to detect resonance. The resonant frequencies, dimensions, and mass of the specimen are used to calculate dynamic Young's modulus.

For reference only, a detailed Campbell Diagram is illustrated on Figure 12 below. It can be noted from Figure 12 that each frequency mode line (horizontal solid and dashed lines in the diagram) is comprised of three lines. These lines represent the cold, hot and ISO day temperature conditions. Also, the rectangular zones near each vibratory excitation driver line (diagonal lines rising from the origin) and the running speed line (vertical line at 3600 RPM mark) intersection represent acceptable margin based on the tuning and the design criteria. The running speed variation zone (two vertical lines near the 3600 RPM mark) is defined and plotted to set the allowable running speed band expected during normal operation. This band is defined in the design criteria as well.

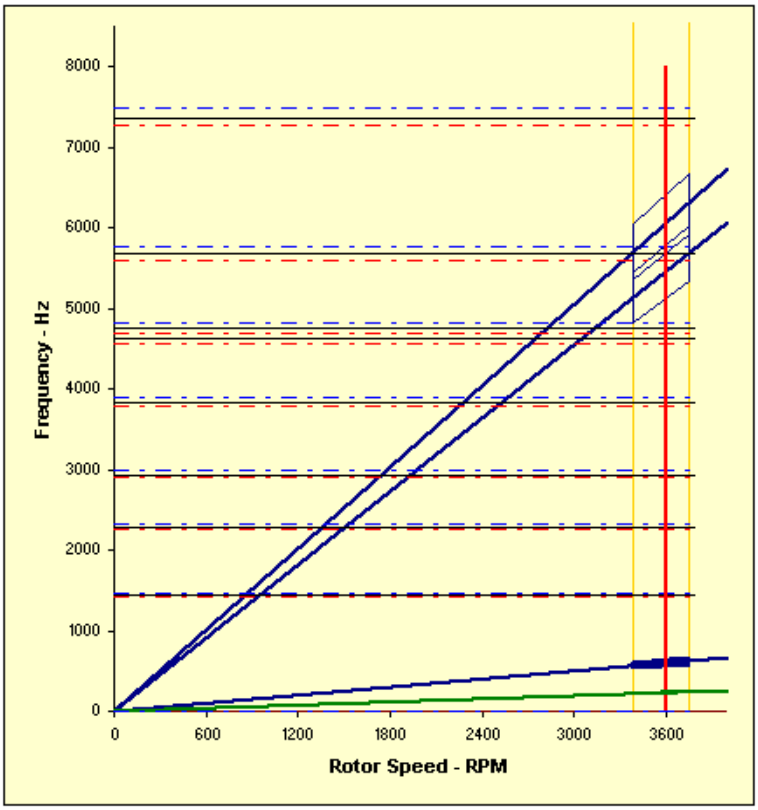


Figure 12. Detailed Campbell Diagram. For reference only.

The actual blade tuning is done by balancing the stiffness and the mass properties of the blade depending on the particular frequency mode. In most cases this process is iterative since the blade properties changes effect the entire spectrum. The basic guidelines for tuning are as follows. In order to lower the particular natural frequency the associated region stiffness must be reduced and / or the mass must be increased. The reverse actions accomplish the opposite result – increase of the mode frequency [1], [2], [3], [4].

# CHAPTER THREE: METHODOLOGY

## Overview: Analysis and Research

This Chapter contains details of the finite element model, the analysis used to study the various blends, and their effect on the compressor blade vibratory characteristics.

The object of all associated analysis and techniques was chosen to be the Row 1 compressor blade of the SWPC W501® frame series Industrial Combustion Turbine. Although for the purposes of this discussion it is not critical what row of what engine is used, it is important to note that in service blades and vanes of the earlier stages are exposed to the so called Foreign Object Damage. The reasons earlier stages are more prone to the sustain damage is that during operation most foreign objects would disintegrate after blade and vane impacts as they travel through the engine. In other words, the physical size of the foreign object would effectively decrease towards the rear stages. Therefore, demonstrating the multi-domain analysis approach on the Row 1 blade is the most logical choice for this research.

There are numerous variations of the compressor blade damage in terms of the damage size and the damage location on the blade. (Confer Appendix A. for the blade damage examples.) It is not feasible to capture each and every possible damage and blend within any reasonable analysis time frame. Therefore, for the purpose of this research it was decided to focus on the

three most common damage locations: Leading Edge (LE) Blend, Trailing Edge (TE) Blend, Tip Blend and combination of the three blends above. In order to reach a fundamental conclusion of this project regarding validity of the multi-domain analysis method, it has been necessary to compare the simulated blend models with those of the true blend modeled in detail. This comparison route is illustrated below in the analysis and research diagram (Figure 13):

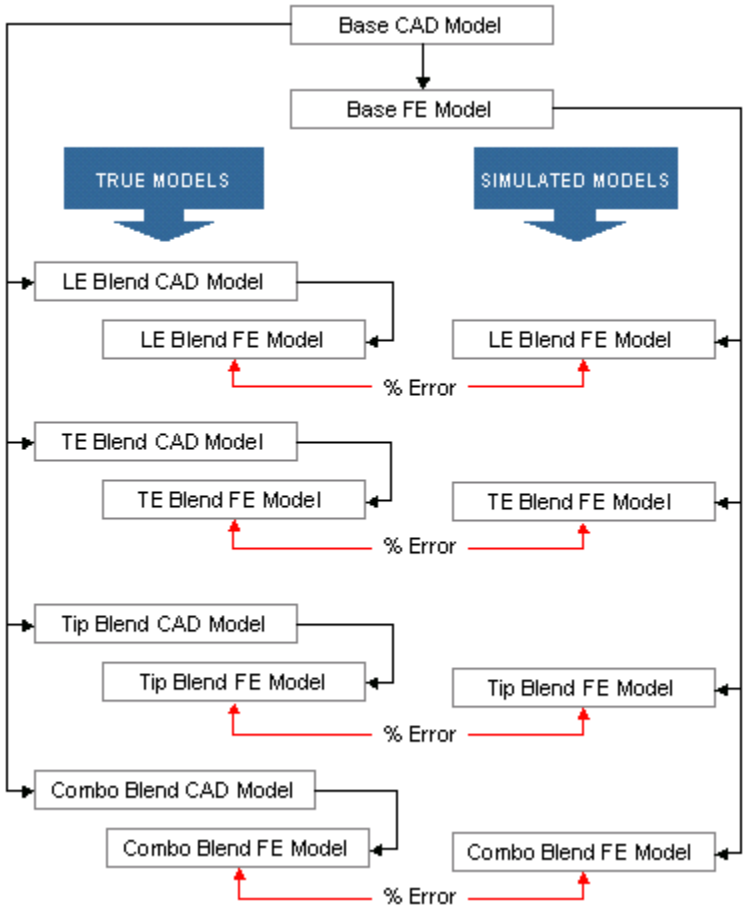


Figure 13. Research Methodology Diagram.

## Finite Element Model Configuration

The Row 1 compressor blade is forged out of 17-4PH Stainless Steel and machined to the final shape. Its overall dimensions are illustrated below on Figure 14:

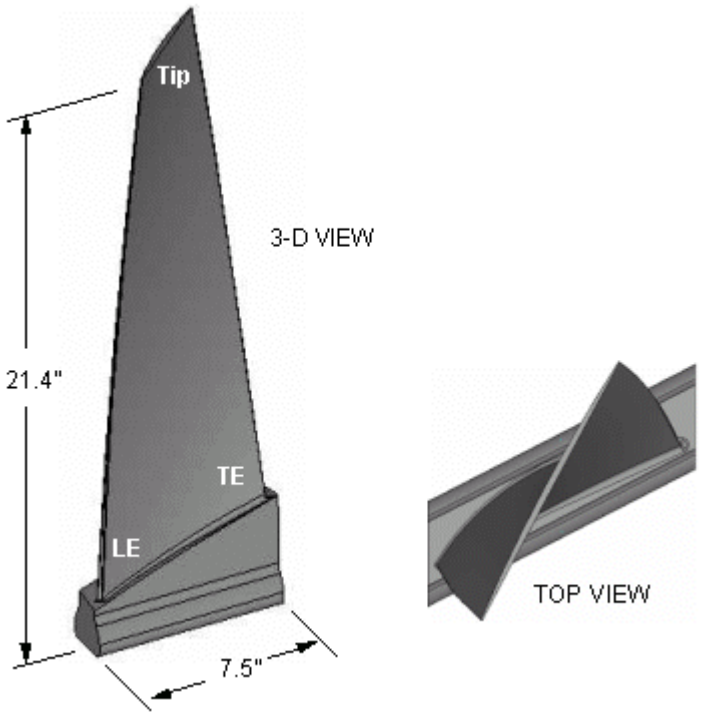


Figure 14. Row 1 Blade Dimensions.

The material and strength properties are given in the table below (Table 1).

Table 1. Blade Material and Strength Properties.

| Material: | 17-4PH (Stainless Steel) | |
|---|---|---|
| Relative inlet temperature: | 100.0 $^0$F | 37.8 $^0$C |
| Dynamic Modulus, E | 2.97E+04 ksi | 2.05E+05 MPa |
| Yield Strength: | 120.8 ksi | 833.40 MPa |
| Ultimate Strength: | 133.0 ksi | 917.50 MPa |
| Endurance Strength: | 59.9 ksi | 412.9 MPa |

The boundary conditions have been established to properly simulate the blade assembled in the rotor disk [4]. The blade root (a.k.a. platform) has the dove tail configuration and it is installed in the corresponding rotor disk slot. This results in the two side surfaces on the blade root to be reacting against the corresponding inside surfaces of the disk slot during operation. The centrifugal force at high RPM values essentially locks the blade into place. The boundary condition type to simulate this effect was chosen to be "fixed restraint" as show below on Figure 15. This figure also shows several blades as installed in the rotor disk, for reference only.

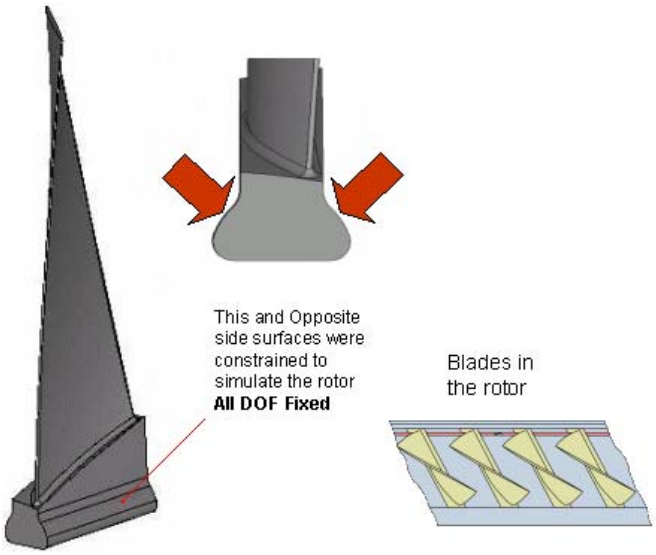


Figure 15. FEM Boundary Conditions.

The boundary conditions illustrated on the Figure 15 above were used for all analysis in this research.

The FEA software code employed was SC03 Version 7C0. This code is developed by Rolls-Royce and is proprietary airfoil analysis code [4].

The FE Model was comprised (on average) of 15,000 Tetrahedral 10-noded Elements which resulted in approximately 30,000 nodes. The photo below illustrates the base model mesh.


Figure 16. Finite Element Model Mesh Views.

Although some models mesh varied slightly the variation was not significant enough to make mention of in this thesis.

Although in general the modal analysis is performed without loading, this case is unique in the sense that the effects of CF stiffening must be taken into account. When the engine is operated at rated speed of 3600 RPM (60 Hz) the centrifugal forces acting on rotating parts are quite high. In case of the compressor blade obviously these forces will depend on the mass and the radius of rotation for a given row of blades. The stiffening effect corrections are built into the code (SC03) which was chosen to run the associated modal analyses. Therefore, no additional calculations were necessary to address the CF stiffening and how it effects the natural frequency values. The output of each analysis run contains two sets of frequency modes: 1)at 0 RPM and 2) at 3600 RPM.

## Model Calibration: Bump Test

In order to calibrate the base finite element model the "free-free" bump test was performed. This results of this test were compared to the free-free finite element modal analysis results. Please, see Appendix C. for the complete bump test details and photographs.

In summary several (two) new blades were suspended on rubber cords in the air. After the bump test equipment and accelerometers were attached and connected the blade was "bumped" using the special hammer electronically connected to the data acquisition equipment. The processed vibration frequencies were plotted to document the results.

Table 2. Bump Test Results.

| # | BLADE 1 | | | BLADE 2 | | | AVG BLADE 1 & 2 | | |
|---|---|---|---|---|---|---|---|---|---|
| | Freq, Hz | | | Freq, Hz | | | Freq, Hz | | |
| | Bump Test free-free Blade | FEA free-free blade | % Delta | Bump Test free-free Blade | FEA free-free blade | % Delta | Bump Test free-free Blade | FEA free-free blade | % Delta |
| **1** | 211.3 | 211.0 | 0.13 | 208.8 | 211.0 | -1.05 | 210.1 | 211.0 | -0.46 |
| **2** | 465.0 | 467.9 | -0.63 | 460.0 | 467.9 | -1.69 | 462.5 | 467.9 | -1.16 |
| **3** | 551.3 | 549.9 | 0.26 | 545.0 | 549.9 | -0.89 | 548.2 | 549.9 | -0.31 |
| **4** | 896.3 | 901.8 | -0.61 | 885.0 | 901.8 | -1.87 | 890.7 | 901.8 | -1.24 |
| **5** | 1008.0 | 1012.5 | -0.44 | 997.5 | 1012.5 | -1.48 | 1002.8 | 1012.5 | -0.96 |
| **6** | 1113.0 | 1108.8 | 0.38 | 1096.0 | 1108.8 | -1.15 | 1104.5 | 1108.8 | -0.38 |
| **7** | 1325.0 | 1339.1 | -1.05 | 1316.0 | 1339.1 | -1.73 | 1320.5 | 1339.1 | -1.39 |
| **8** | 1665.0 | 1672.4 | -0.44 | 1653.0 | 1672.4 | -1.16 | 1659.0 | 1672.4 | -0.80 |
| **9** | 1759.0 | 1771.5 | -0.71 | 1746.0 | 1771.5 | -1.44 | 1752.5 | 1771.5 | -1.07 |
| **10** | 1818.0 | 1842.9 | -1.35 | 1811.0 | 1842.9 | -1.73 | 1814.5 | 1842.9 | -1.54 |

The resultant correlation showed a maximum of 1.54% error for Modes 1-10 and a max of 1.24% error for Modes 1-6. This was deemed acceptable for further analysis of this model and for use of the same mesh size and quantity for all subsequent models as well.

Next the analysis and the models layout was established in order to confirm the principal of the multi-domain simulation.

## Analysis and Blends Layout

As discussed in the Overview section of this Chapter, the simulated the true blends were compared with respect to the natural frequency values. In order to establish a decent statistical correlation it was chosen to create a total of four models for the simulated and the true blends: three separate blends and one combination of all three blends. This approach provided a total of 24 % error data points for the final distribution study (please, see Chapter IV for results). The diagram on Figure 17 illustrates the blends layout and associated dimensions. Table 3 below contains blends location and sizing information.

Table 3. Blends Layout and Details.

| # | **Blend ID** | **Location on Blade** | **Length** | **Depth** |
|---|---|---|---|---|
| **1** | Blend 1 | Leading Edge | 76.2 mm [3.0 in] | 12.7 mm [.50 in] |
| **2** | Blend 2 | Trailing Edge | 102 mm [4.0 in] | 27 mm [1.06 in] |
| **3** | Blend 3 | Tip, Trailing Edge | 101 mm [4.0 in] | 48 mm [1.9 in] |
| **4** | Combination | Blends 1, 2 & 3 | N/A | N/A |

The size and the location of blends on the airfoil were arbitrarily chosen to capture the most common blends and blends combination observed in the field. Also, the proposed layout presented a reasonable mass and stiffness variations in terms of the blade properties – all to illustrate the point of this study.

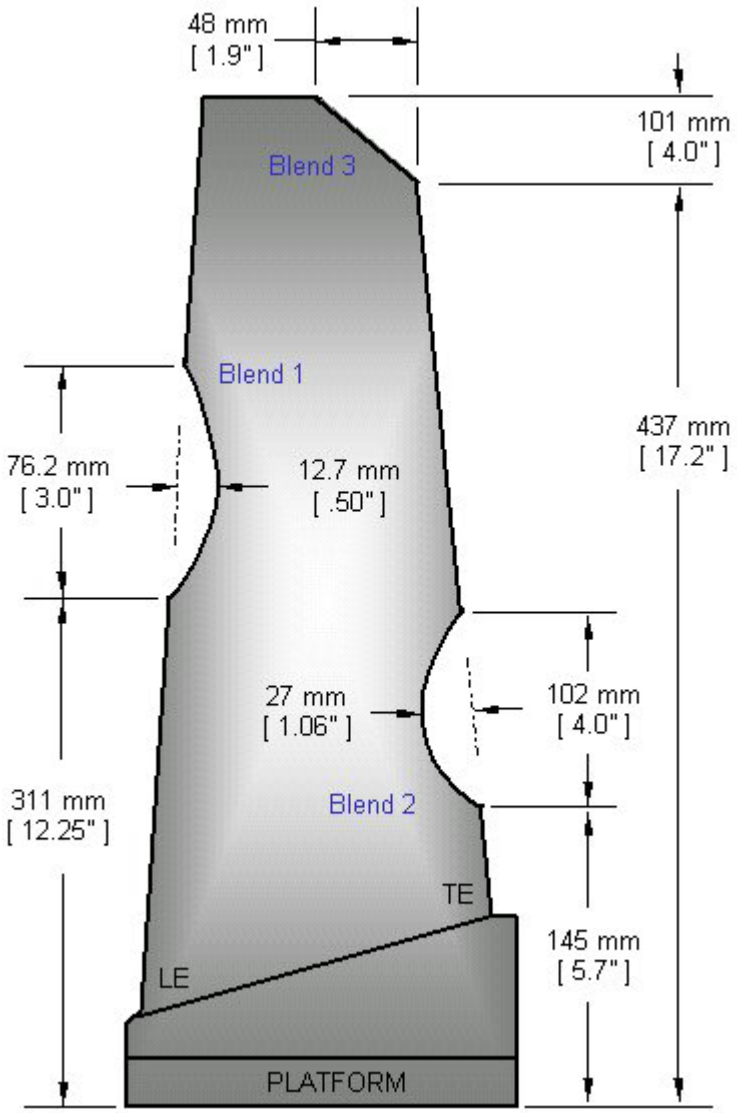


Figure 17. Blends Layout.

The Figure 17 above shows all blends on the same diagram. However, the simulated and the true blend analyses were performed on each blend separately as well as on the combination of all three blends. Together with the base model and the calibration “free-free” model the study

consisted of 10 analyses.

## Multi Domain Setup

The key to the multi-domain concept as it is applied to the modal analysis is to alter the material properties thereby simulating the blend. In this case each simulated blend model contained two domains: base metal domain and blend domain. The two material properties which affect the dynamic behavior are stiffness and mass. The table below (Table 4) demonstrates how the material properties were altered for the second (blend) domain to simulate the blended location on the original FE Model. Density and Dynamic Modulus of Elasticity were both decreased by factor of 100. The natural frequency is proportional to the ratio: $\sqrt{\frac{E}{\rho}}$ and reducing both quantities by the same factor preserved this ratio.

Table 4. Multi-Domain FE Model Material Properties.

| **Material Property** | **Base Domain Value Domain 1** | **Blend Domain Value Domain 2** |
|---|---|---|
| Density ($Kg/m^3$) | $7.80 \times 10^3$ | $7.80 \times 10^1$ |
| Dynamic Modulus of Elasticity (MPa) | $2.06 \times 10^5$ | $2.06 \times 10^3$ |

The different domain properties were applied by selecting appropriate elements on the screen simulating the size and the location of a given blend. Through the software, the material

properties were assigned to each domain as indicated on Table 4 above. The important note to make here is that the element sizing did not land itself to forming the precise smooth outline of the blend yet the results indicated acceptable correlation of natural frequency values between the true and the simulated (multi-domain) models in all cases.

The modifications of material properties described above (by factor of 100) yielded acceptable results during this study. It is possible that there may be other values by which the density and the modulus are changed to simulate the blend. This thesis is only focused on proposing the method of varying the properties, the actual variation may be different for each situation, as dictated by associated analysis and components in question.

Figure 18 below illustrates the multi-domain layout on the FE model for the case of blend combination study. See Appendix D. for more FE Model views.

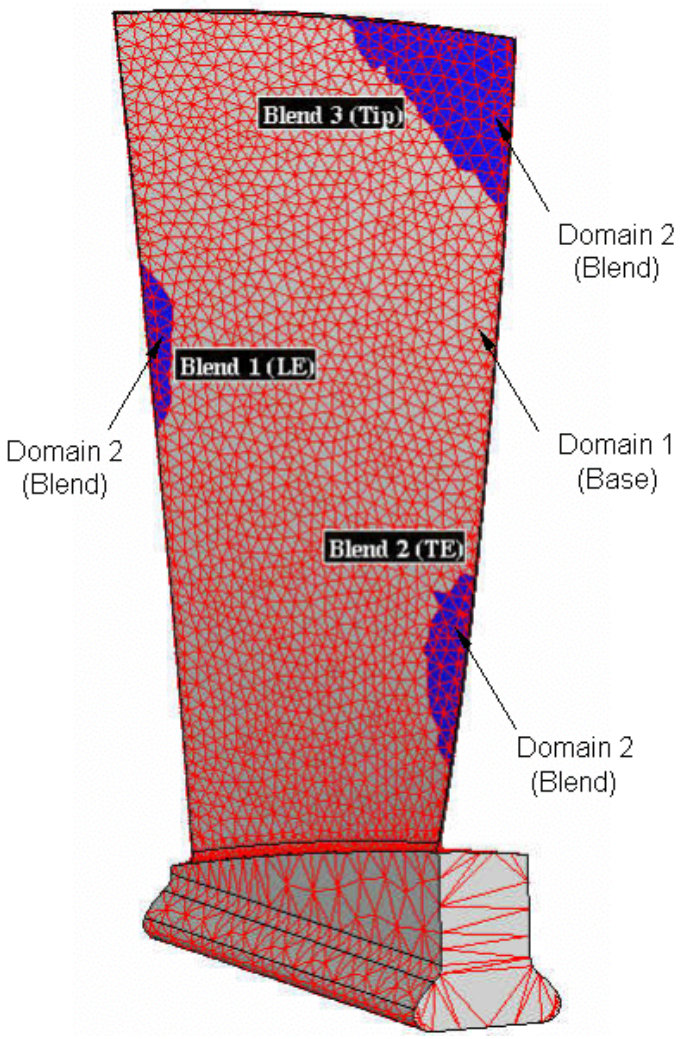


Figure 18. Multi-Domain FE Model Illustration.

# CHAPTER FOUR: RESULTS

This Chapter contains results of all analyses within this study as well as correlation between the true and the simulated models.

## Mode Shapes

No differences in mode shapes were observed between the true, the base and the simulated blend models. The typical mode shapes are illustrated below.

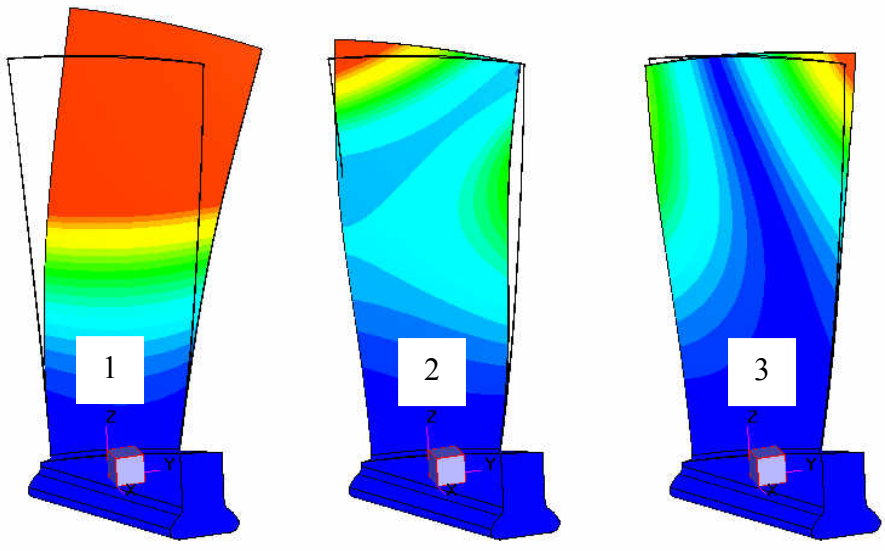


Figure 19. Base Model. Modes 1-3.

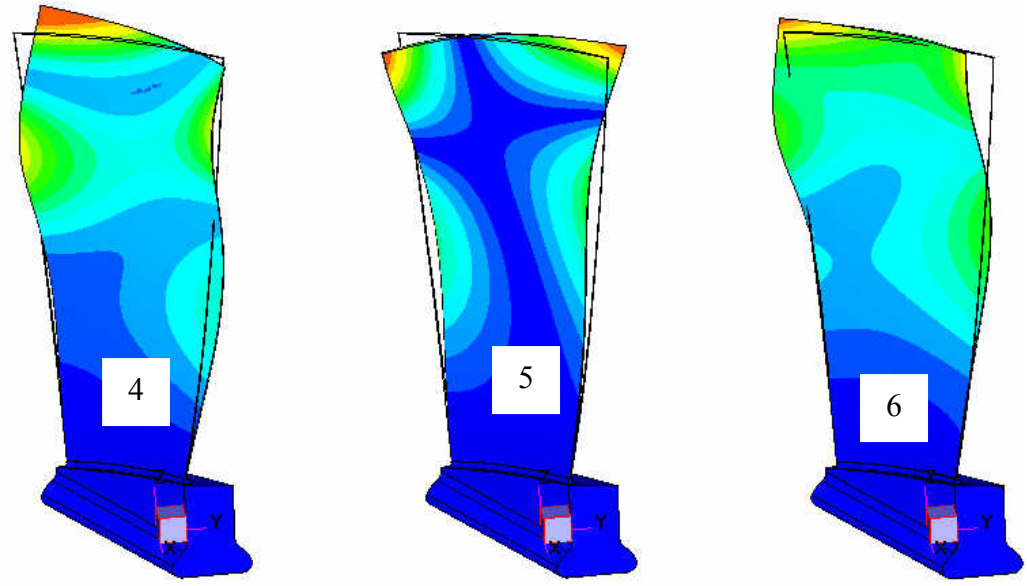


Figure 20. Base Model. Modes 4-6.

The table below contains mode frequencies.

Table 5. Base Model Natural Frequencies.

| Mode | Hz |
|---|---|
| 1 | 145.2 |
| 2 | 366.7 |
| 3 | 436.4 |
| 4 | 744.5 |
| 5 | 886.3 |
| 6 | 955.2 |

## Simulated Blend Models vs. Base Model

After the analyses of the simulated blends were completed, the first six mode frequencies were compared to the base model values. The results of this comparison are illustrated in the table and charts below.

Table 6. Simulated Blend Model Frequencies vs. Base Model Frequencies.

| Mode | Base | Sim. Blend 1 | % delta | Sim. Combo | % delta | Sim. Blend 2 | % delta | Sim. Blend 3 | % delta |
|---|---|---|---|---|---|---|---|---|---|
| 1 | 145.2 | 145.3 | 0.0 | 149 | 2.6 | 144.4 | -0.6 | 150 | 3.3 |
| 2 | 366.7 | 367.0 | 0.1 | 367 | 0.1 | 366 | -0.2 | 368 | 0.4 |
| 3 | 436.4 | 434.7 | -0.4 | 491 | 12.5 | 430 | -1.5 | 501 | 14.8 |
| 4 | 744.5 | 748.3 | 0.5 | 760 | 2.1 | 745 | 0.1 | 755 | 1.4 |
| 5 | 886.3 | 892.0 | 0.6 | 929 | 4.8 | 876 | -1.2 | 946 | 6.7 |
| 6 | 955.2 | 957.2 | 0.2 | 965 | 1.0 | 930 | -2.6 | 986 | 3.2 |

The *%delta* was calculated as follows:

$$\%delta = \frac{(blend - base)}{base} \cdot 100\% \text{ (all Hz values)}$$

It is interesting to note the large percentage changes for Modes 3 and 5 within the Simulated Blend 3 and Combination (combo) models. See Figure 17 for blends layout and identification.

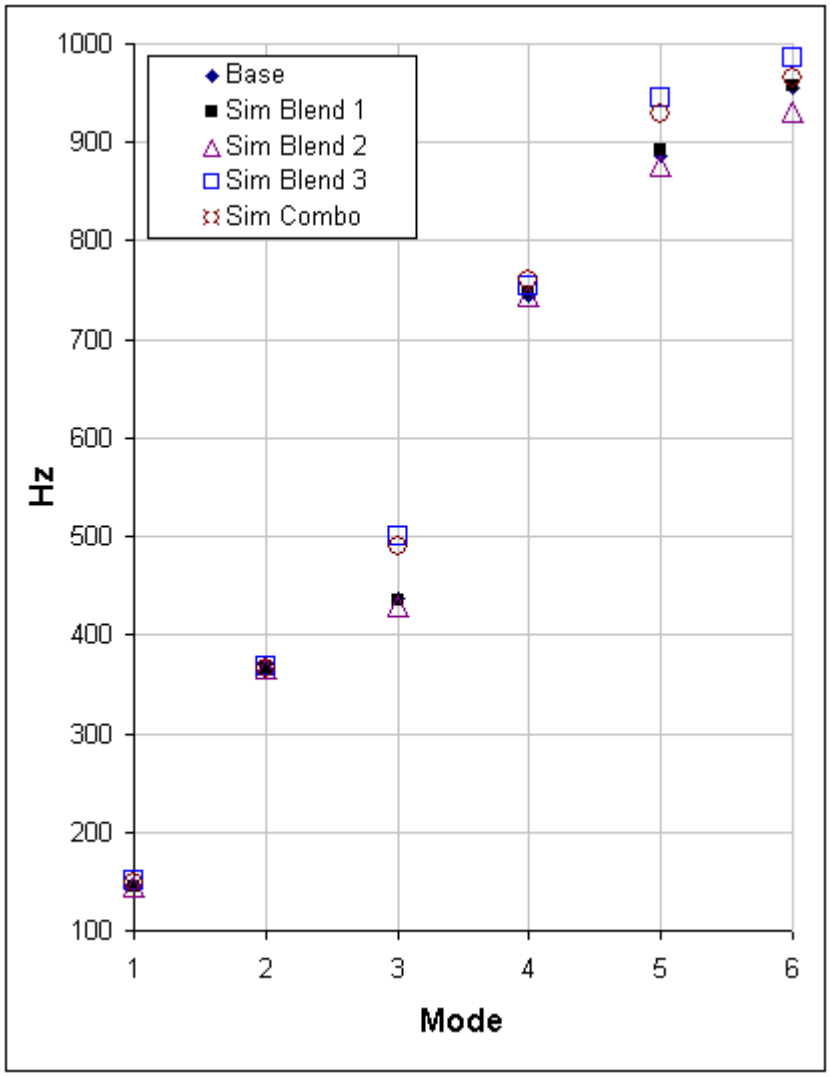


Figure 21. Frequency Values: Simulated Blend Models vs. Base Model.

In order to "zoom in" on areas of differences in frequency values, the graph on Figure 21 has been split into two separate graphs as shown on the following pages, Figure 22 and Figure 23.

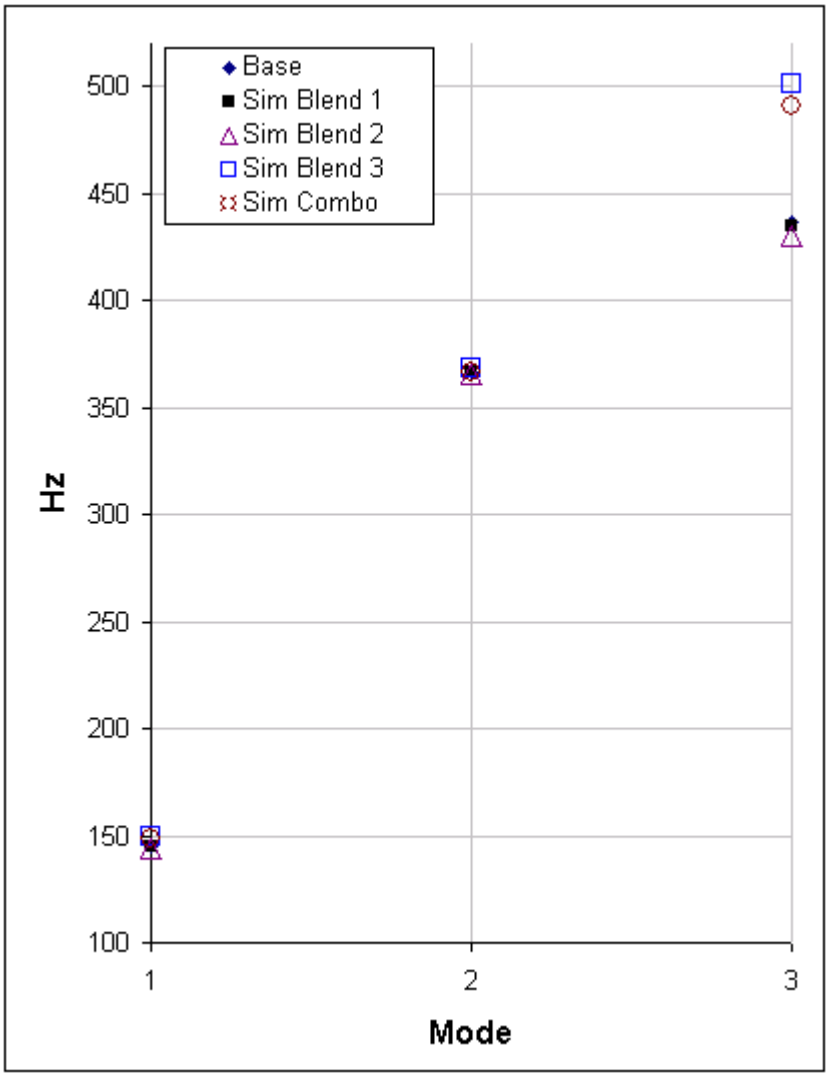


Figure 22. Modes 1-3: Simulated Blend Models vs. Base Model.

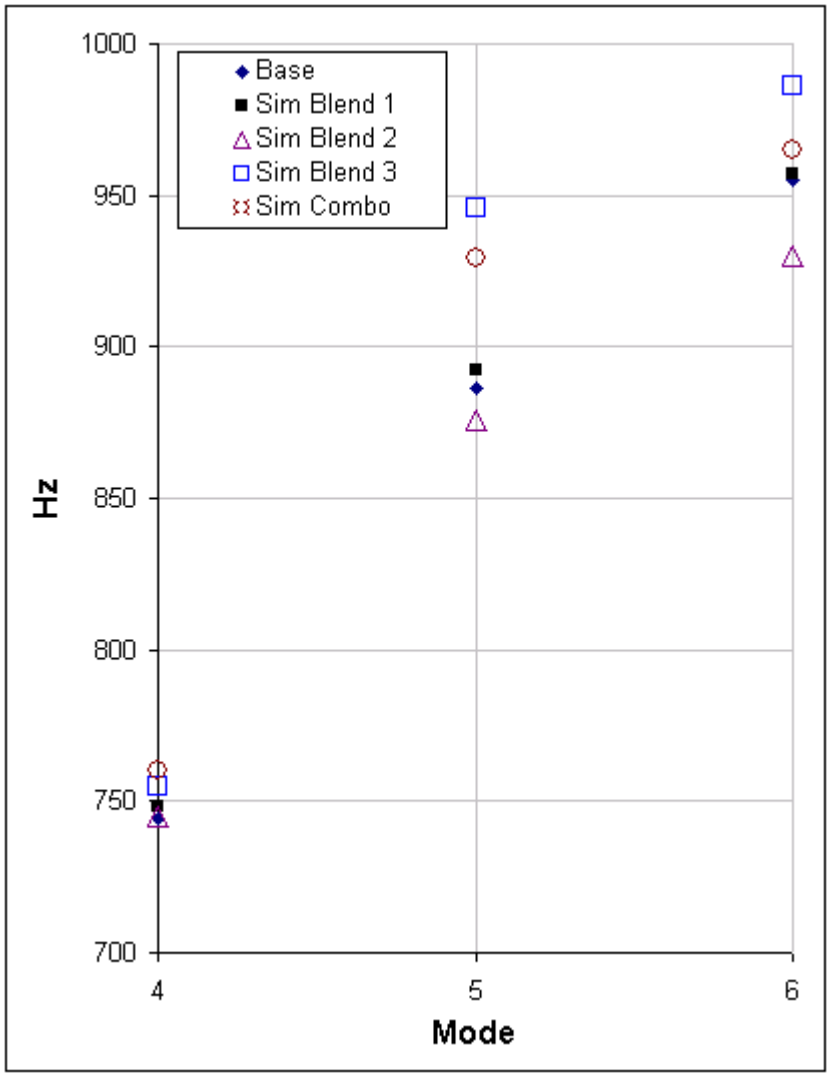


Figure 23. Modes 4-6: Simulated Blend Models vs. Base Model.

## Simulated Blend Models vs. True Blend Models

Continuing with the main topic of this thesis (multi-domain blend simulation technique), this section contains a comparison of the multi-domain simulated blend models with the true blend FE models. Figure 24 below illustrates the true blend FE models.

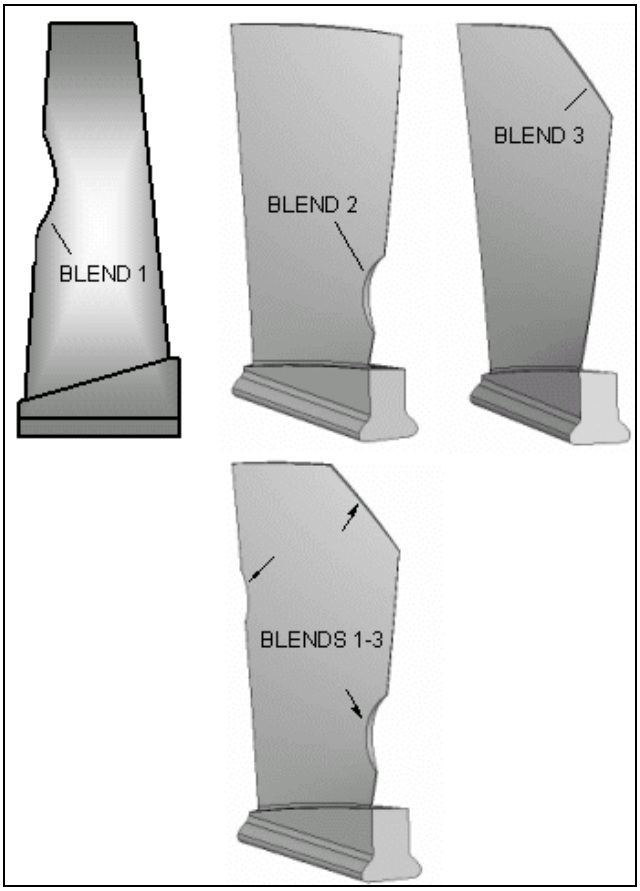


Figure 24. True Blend Finite Element Models. Blend 1, 2 & 3.

Figure 25 below illustrates finite element model meshed view.

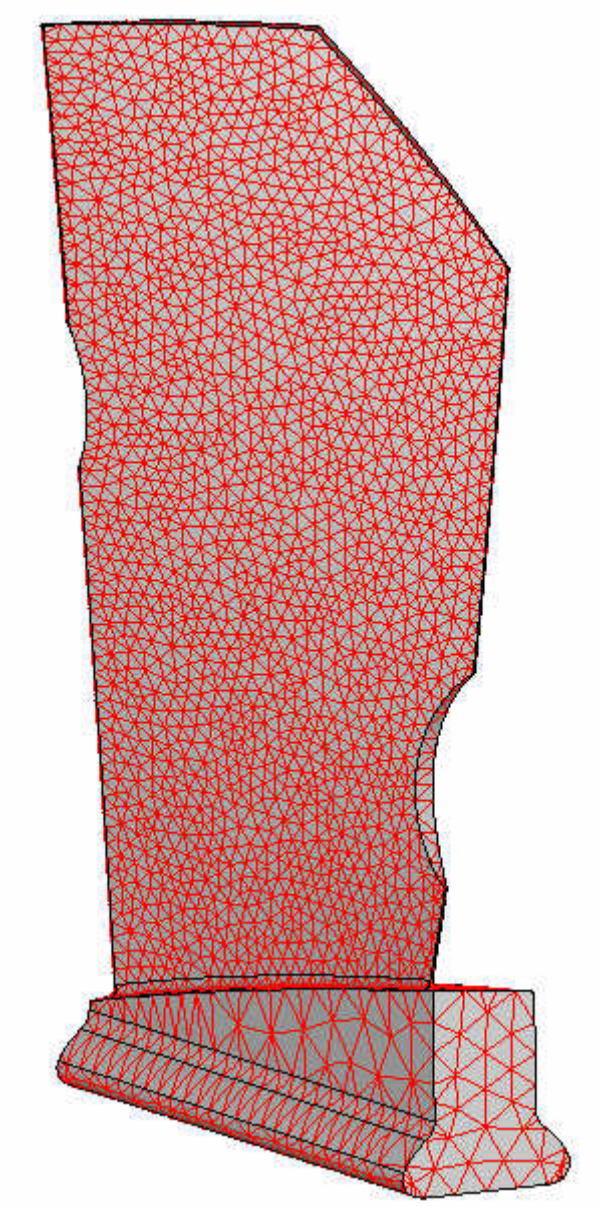

Figure 25. True Blends 1-3 (combination) model. Meshed.

The modal analyses of all models described and shown above were performed to

determine the first six frequency values. Once determined, these values were compared between the true blend FE models and the simulated multi-domain blend models. The table below (Table 7) contains results of this comparison.

Table 7. Simulated vs. True Blend Frequency Results.

| Mode | Blend 1 | | | Blend 2 | | |
|---|---|---|---|---|---|---|
| | **True** | **Simulated** | **% error** | **True** | **Simulated** | **% error** |
| **1** | 145.33 | 145.28 | -0.03 | 144.40 | 144.65 | 0.17 |
| **2** | 367.08 | 367.00 | -0.02 | 366.00 | 365.72 | -0.08 |
| **3** | 434.56 | 434.70 | 0.03 | 430.00 | 432.03 | 0.47 |
| **4** | 748.83 | 748.30 | -0.07 | 745.00 | 745.82 | 0.11 |
| **5** | 890.74 | 892.00 | 0.14 | 876.00 | 879.54 | 0.40 |
| **6** | 956.41 | 957.20 | 0.08 | 930.00 | 934.54 | 0.49 |
| | | | | | | |
| **Mode** | **Blend 3** | | | **Combination (Blends 1-3)** | | |
| | **True** | **Simulated** | **% error** | **True** | **Simulated** | **% error** |
| **1** | 150.00 | 149.74 | -0.17 | 149.00 | 149.14 | 0.09 |
| **2** | 368.00 | 368.34 | 0.09 | 367.00 | 367.00 | 0.00 |
| **3** | 501.00 | 500.00 | -0.20 | 491.00 | 494.12 | 0.64 |
| **4** | 755.00 | 756.00 | 0.13 | 760.00 | 757.80 | -0.29 |
| **5** | 946.00 | 943.30 | -0.29 | 929.00 | 934.62 | 0.60 |
| **6** | 986.00 | 983.90 | -0.21 | 965.00 | 965.34 | 0.04 |

A total of 24 data points of %error comparison were obtained. This data was plotted on a histogram diagram to determine the statistical mean and median of percent error for the proposed multi-domain method study. The statistical summary is presented in Figure 26. Also, see Appendix F for additional percent error correlation statistical data, and Appendix E for FEA model views.

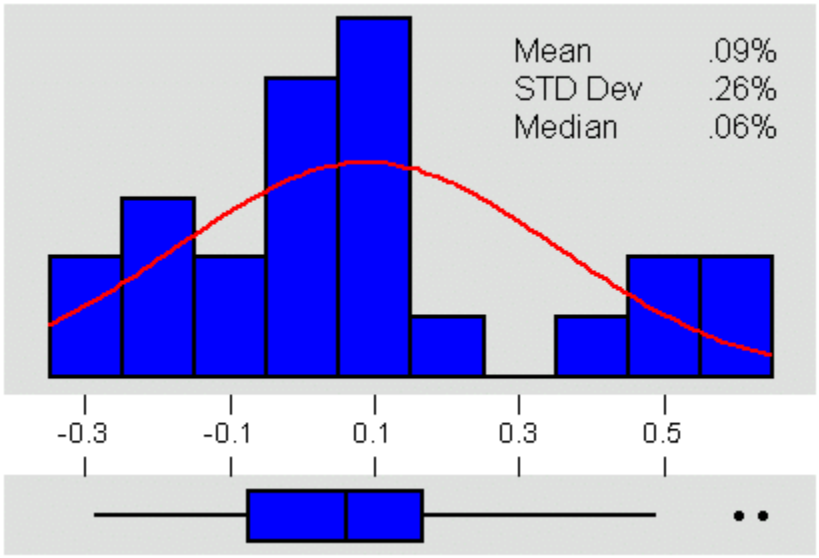


Figure 26. Statistical Correlation Summary, %error.

# CHAPTER FIVE: CONCLUSIONS AND RECOMMENDATIONS

The presented thesis has studied a proposed method of compressor blade damage blend evaluation via multi-domain model simulation. The method has been determined to be accurate and time efficient. The overall accuracy of multi-domain simulated models has been determined to be 0.09% error where the worst percent error has been calculated at 0.60%.

It is recommended that this method be used in the cases in which modal analysis is required to determine the effect of blended-out material on vibratory properties of a compressor blade. The time efficiency of the proposed method is claimed based on the fact that no additional CAD and FEA models were required to simulated the blend for the modal analyses. Therefore, the time required for the cycle of additional CAD and FEA models creation can be spent on other tasks at hand.

This thesis is only focused the affect of the blend on the vibratory properties of the blade. Other aspects of blade design such as stress, aero-flow and balance must be considered for each blend case.

For the future research it is suggested to complete the following studies:

- Through analysis iterations determine the optimum multi-domain elements material properties. This should be done to optimize the computer time vs. accuracy ratio to

further improve the turn-around decision cycle time.

- Applicability of the Multi-Domain method for other turbine components.

# APPENDIX A:
# COMPRESSOR BLADE DAMAGE PHOTOGRAPHS

Figure 27A. Compressor Blade Damage Example 1.

Figure 28A. Compressor Blade Damage Example 2.

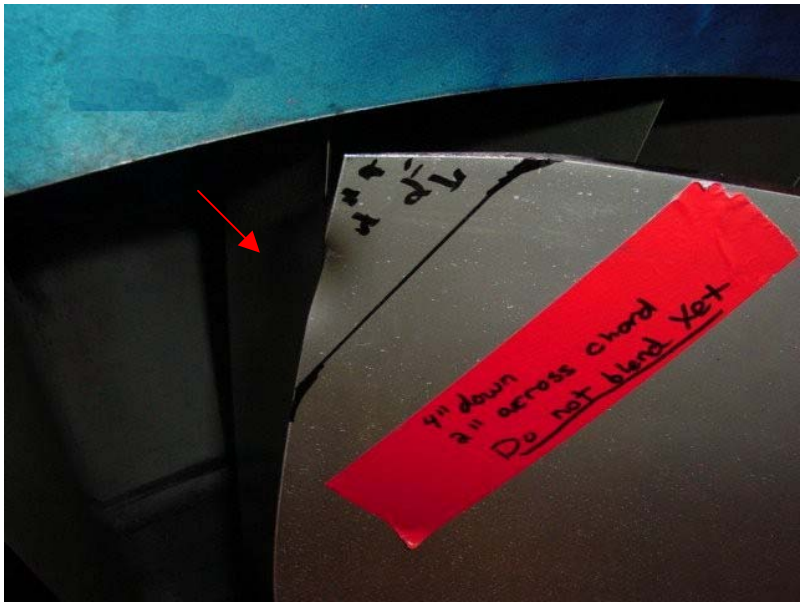


Figure 29A. Compressor Blade Damage Example 3.

Figure 30A. Compressor Blades Blended Example.

# APPENDIX B:
# INLET CYLINDER PHOTOGRAPHS

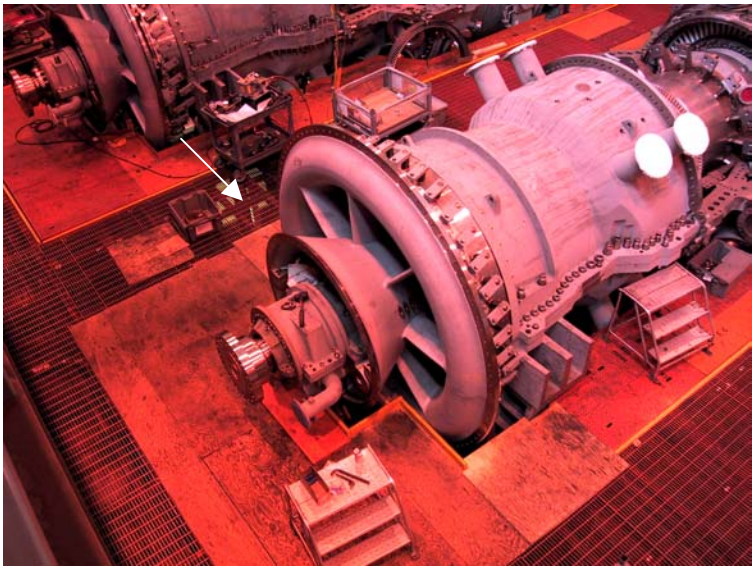

Figure 31A. Inlet Cylinder Assembled.

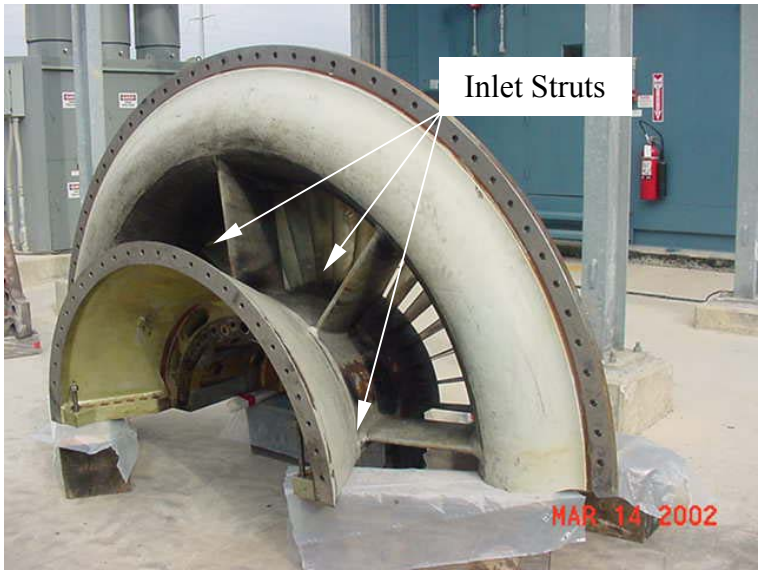


Figure 32A. Inlet Cylinder Cover Removed.

# APPENDIX C:
# BUMP TEST REPORT

The text and photos in the Appendix C contain the Bump Test Report of the Row 1 compressor blade.

**SUBJECT:** Ping testing of two W501D5A row 1 compressor blades.

**DESCRIPTION:** Perform frequency response impact tests on two discrete D5A row 1 compressor blades, identified as: Sample No.1 and Sample No.2. compressor blades are not identified with serial numbers.

***Requested by:*** *Gennadiy Afanasiev* ***Copies to:*** *G. Afanasiev* *Q1-267*

**1. *Background:***

Two new randomly selected D5A row 1 blades were pulled from stores in order to perform a free-free bump test and quantify the first six modal frequencies.

**2. *Test Setup:***

The following equipment was used in performing the frequency response impact test.

- Spectral Dynamics, Signal Analyzer, m/n 2300-9722
- Dell, Controller, m/n 7500
- PCB, Modal Hammer, m/n 086B01
- Endevco, Miniature Accelerometer, m/n 2250A-10
- Zonic Book, eZ-Analyst Software

Frequency response data from each of the blades was acquired while the blade was in a 'free-free' test condition, suspended in space from two elasticized shock cords.
The cross transfer function (CTF) data collection measurement method was used, in an attempt to document all of the natural frequencies present in the vane. The impact point was located on a grid that was 2.5" downstream from the leading edge and 13.5" down from the tip, while the response point was located inward from the trailing edge tip on a 1" by 1" grid. The excitation and response locations were consistent for both test blades. The following Fig. 1 displays the blade test setup with the impact and response locations.

Figure 33A. Bump Test Report. Page 1.

Figure 34A. Bump Test Report. Page 2.

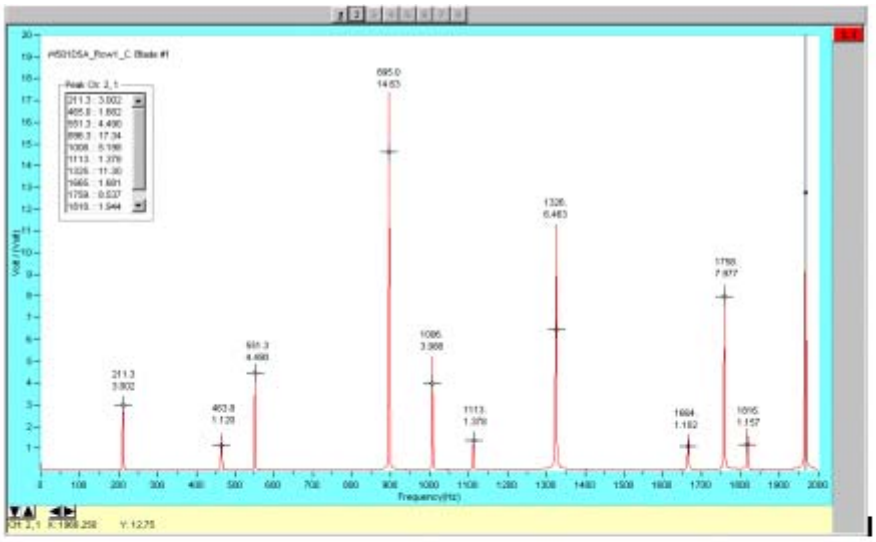

Blade Sample No.1 @1600 Spectral Lines

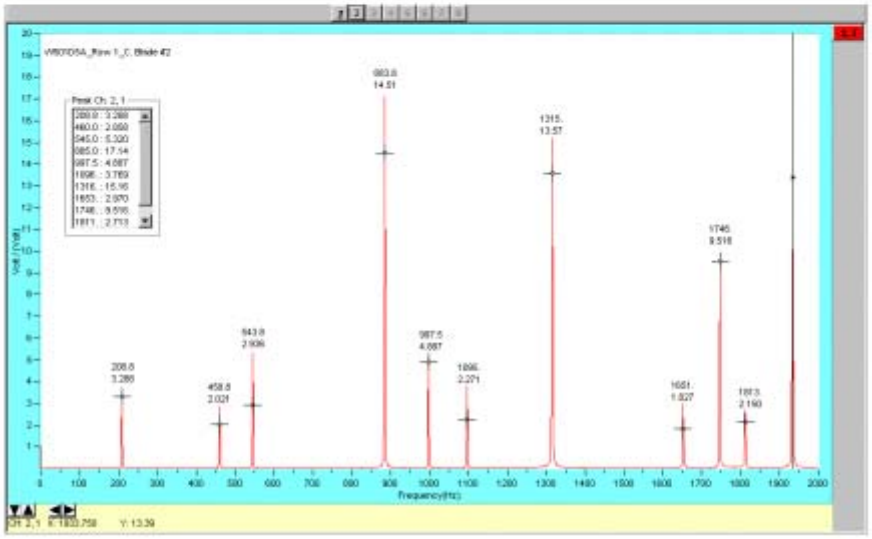

Blade Sample No.2 @1600 Spectral Lines

Figure 35A. Bump Test Report. Page 3.

# APPENDIX D:
# FINITE ELEMENT MODEL VIEWS


Figure 36A. Blend 1 Simulation.

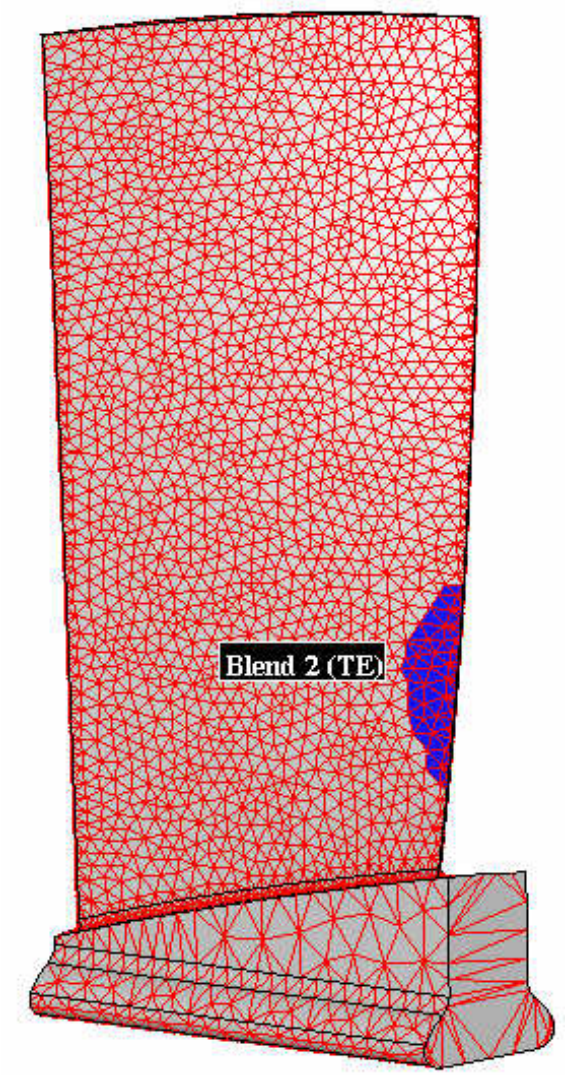


Figure 37A. Blend 2 Simulation.

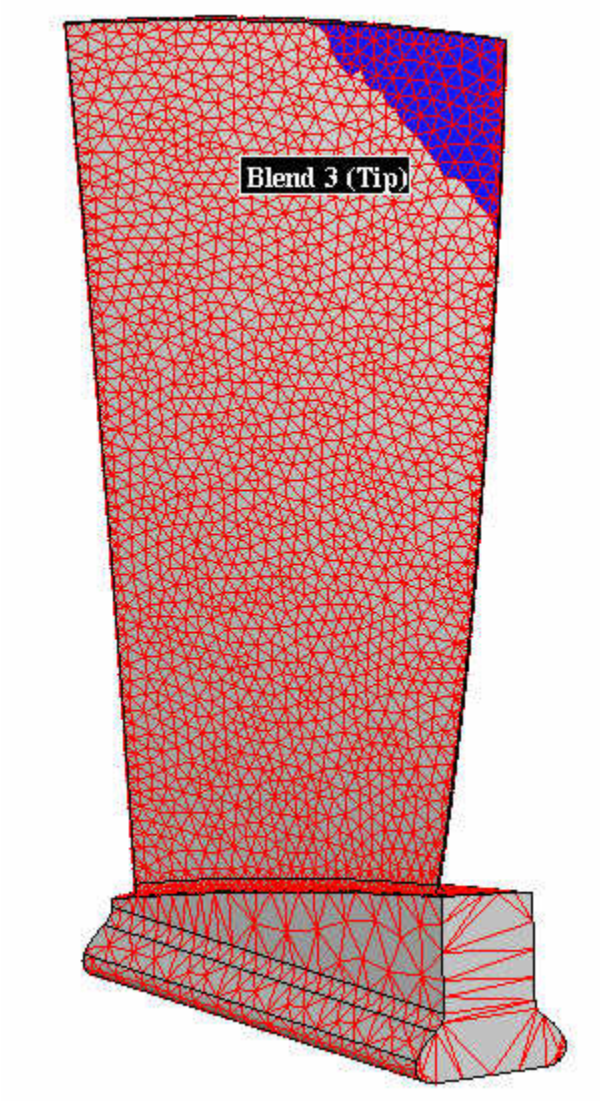


Figure 38A. Blend 2 Simulation.

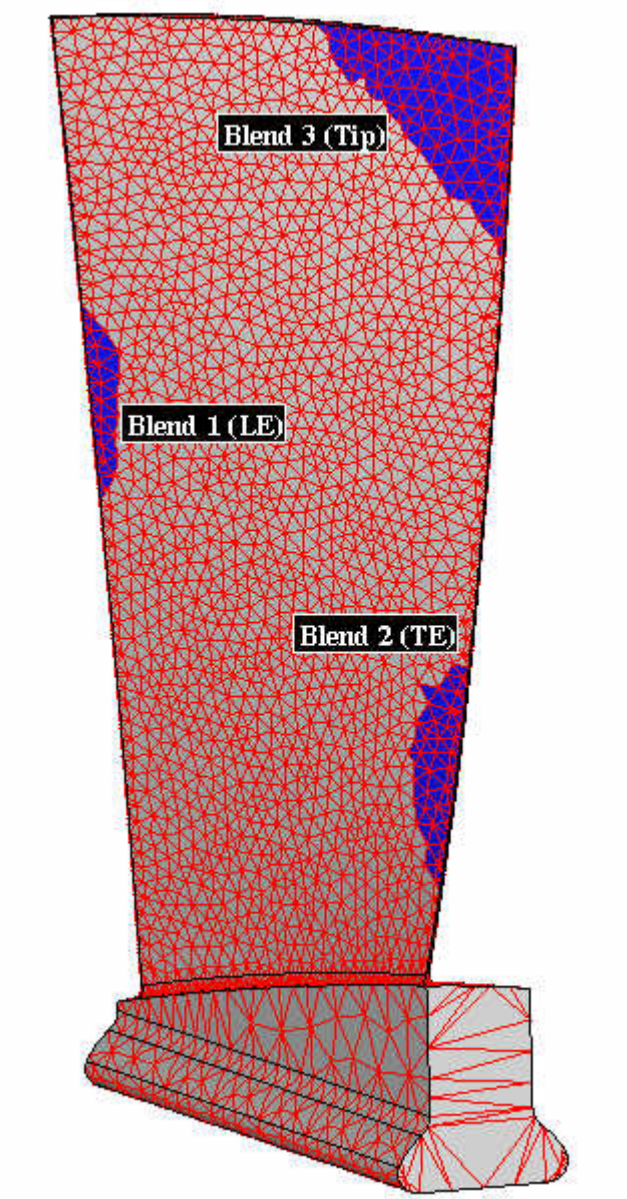


Figure 39A. Combination of Blends 1-3 Simulation.

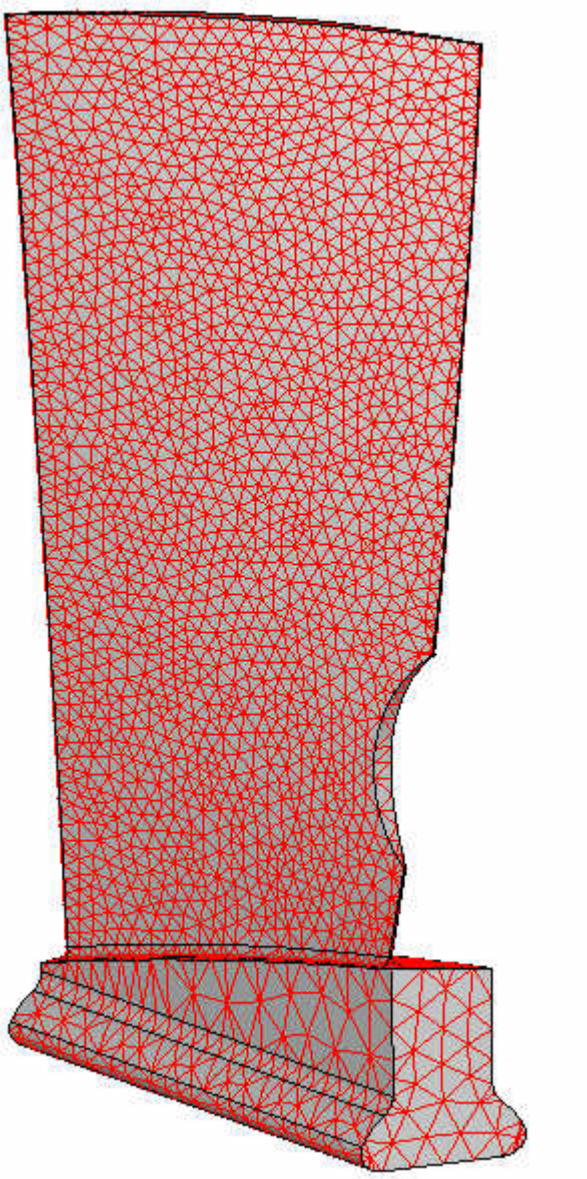

Figure 40A. True Model of Blend 2.

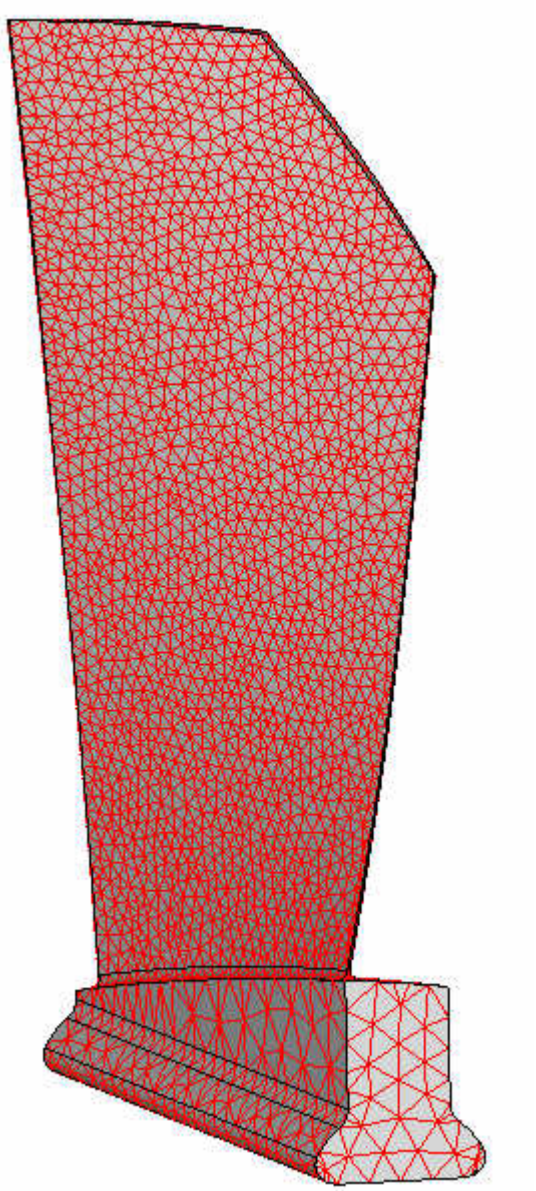

Figure 41A. True Model of Blend 3.

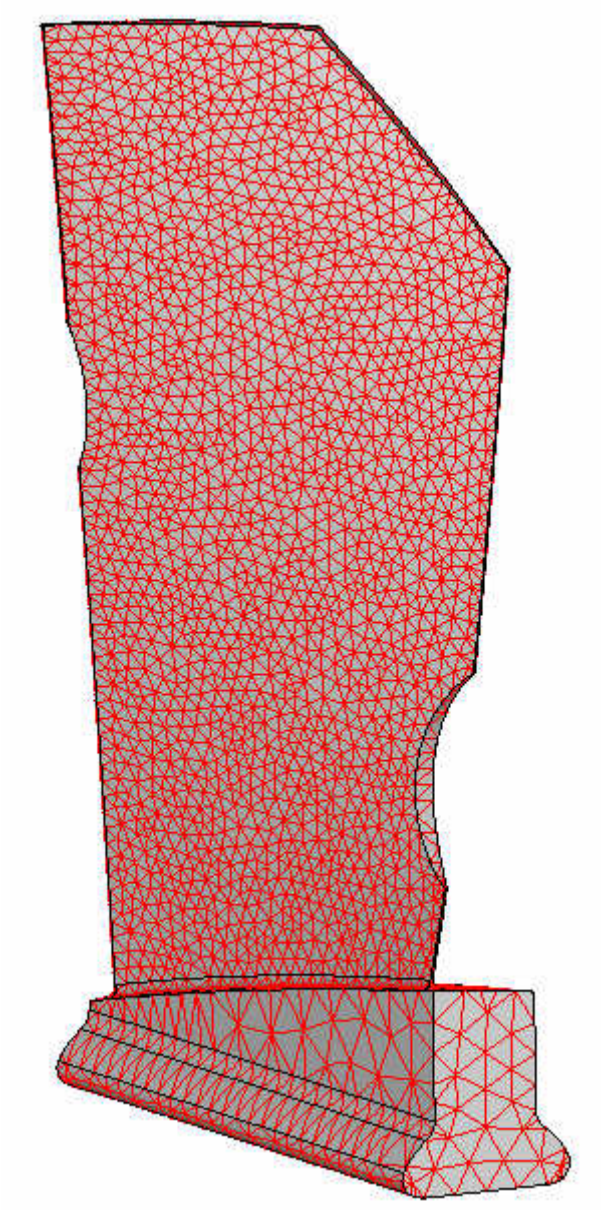

Figure 42A. True Model of Blends 1-3 (combination).

# APPENDIX E:
# CAMPBELL DIAGRAMS (HZ VS. ENGINE SPEED)

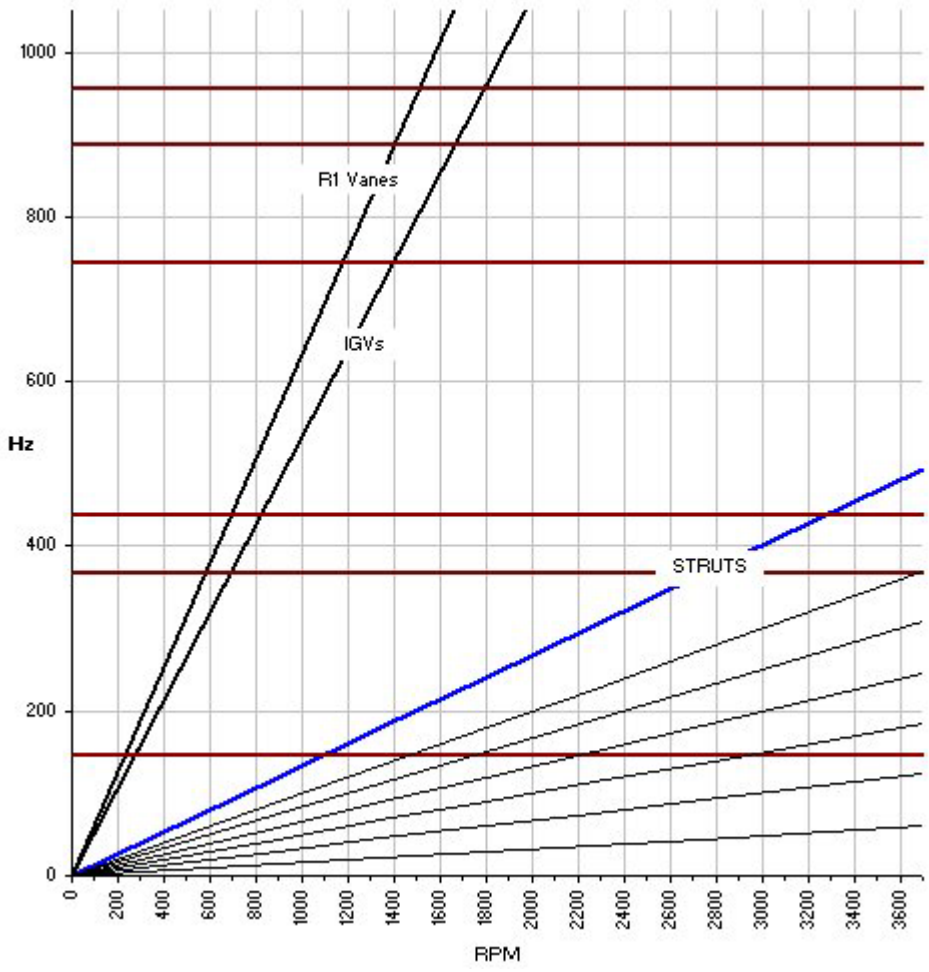


Figure 43A. Base Model Campbell Diagram.

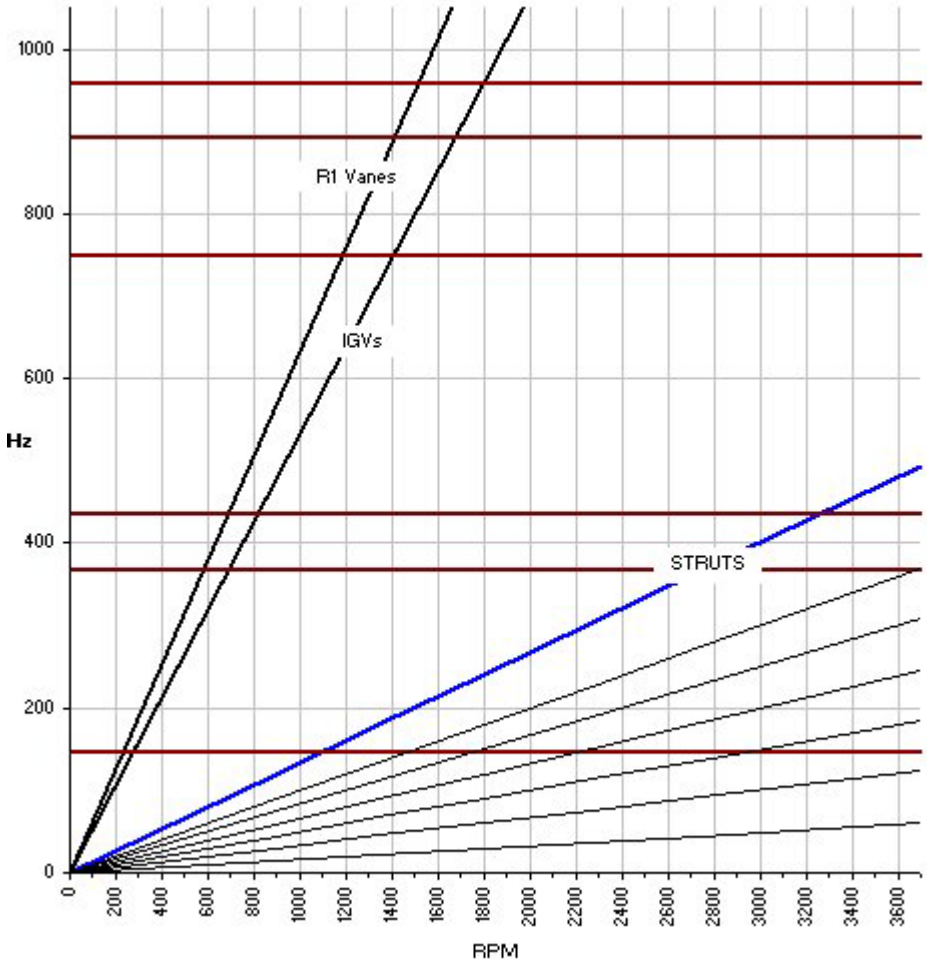


Figure 44A. Blend 1 (Leading Edge) Campbell Diagram.

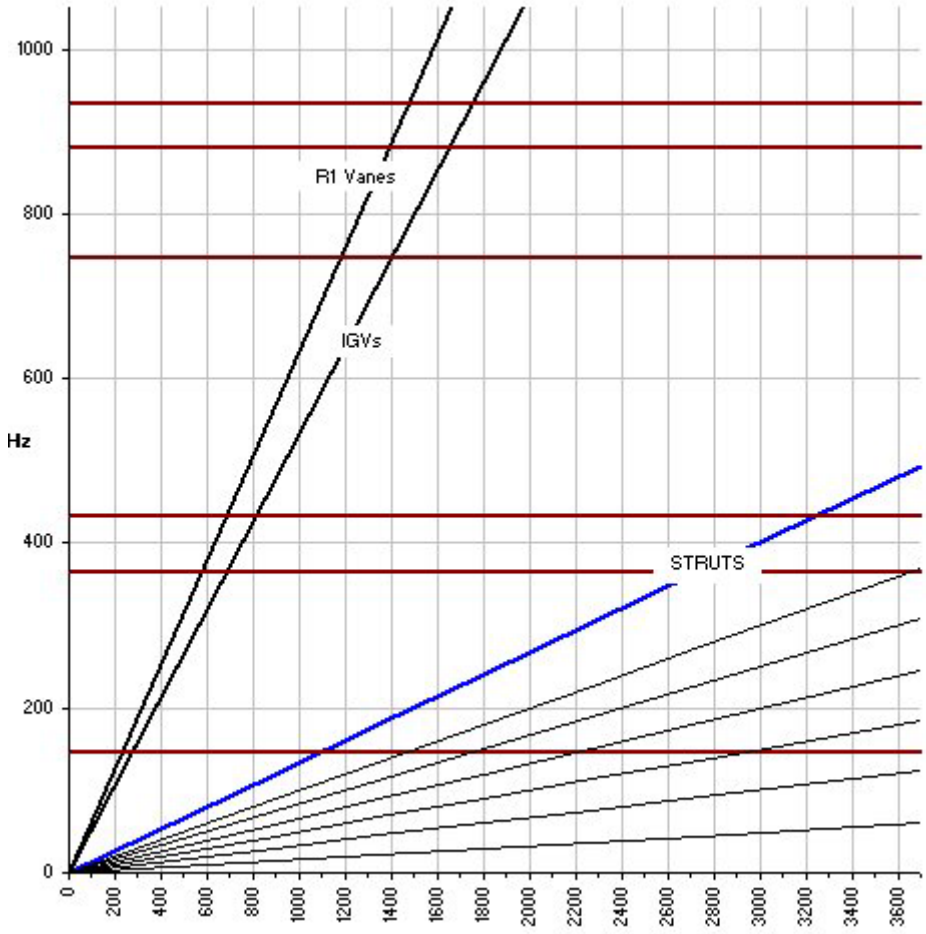


Figure 45A. Blend 2 (Trailing Edge) Campbell Diagram.

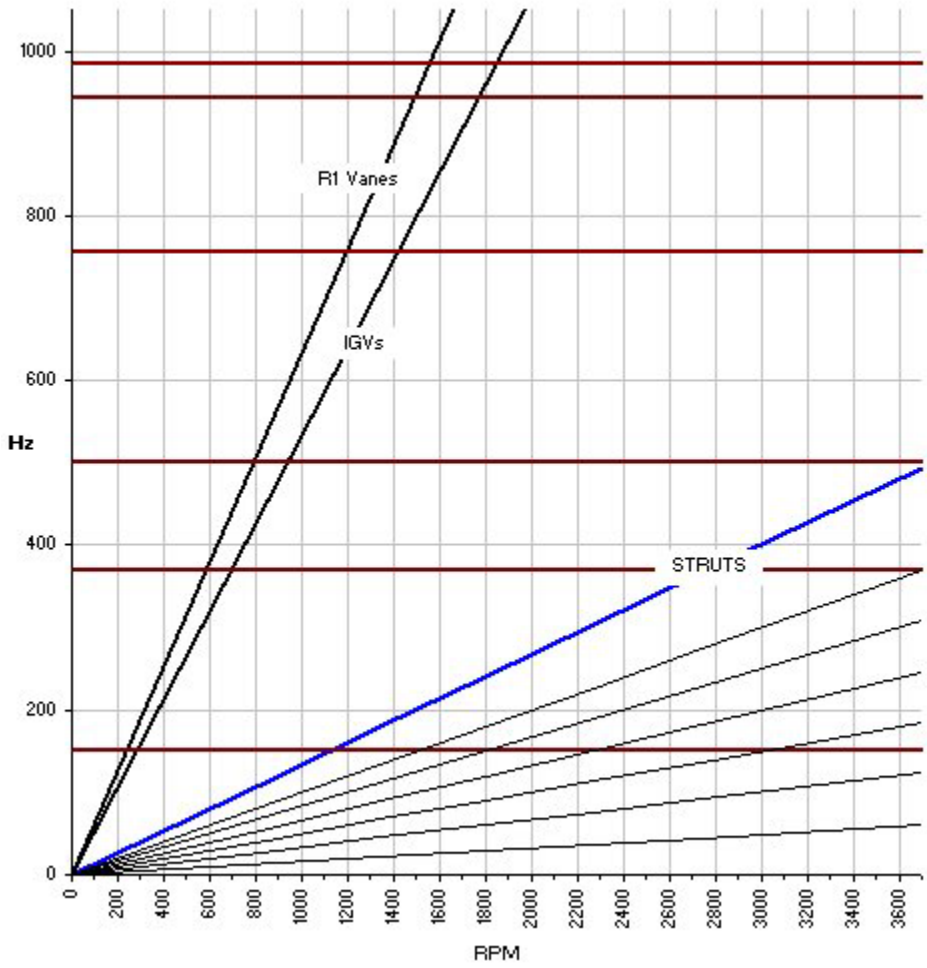


Figure 46A. Blend 3 (tip) Campbell Diagram.

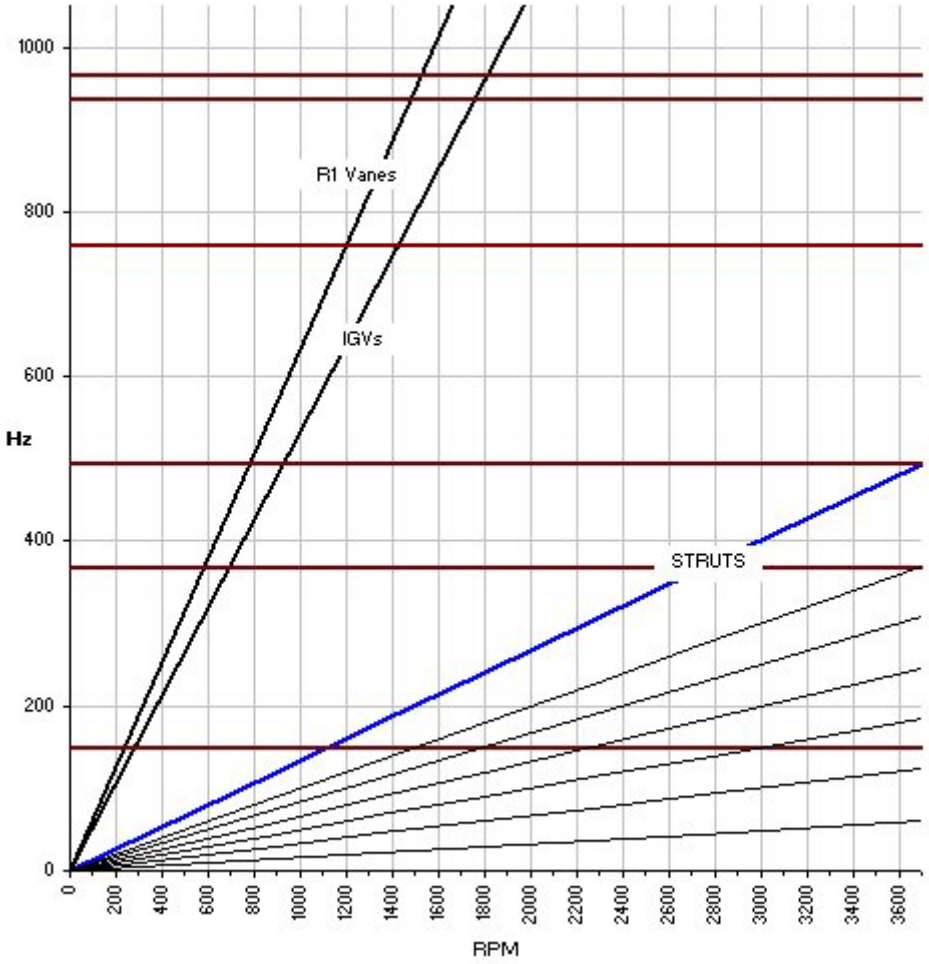


Figure 47A. Blends 1-3 (combination) Campbell Diagram.

# APPENDIX F:
# STATISTICAL REVIEW OF CORRELATION RESULTS

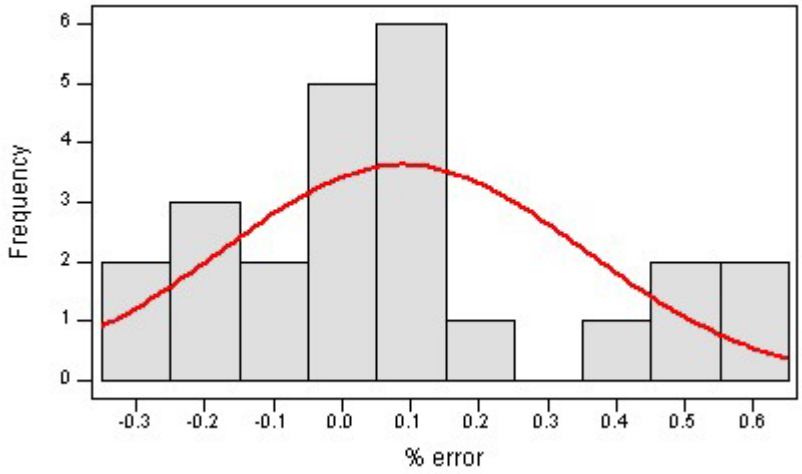


Figure 48A. Percent Error Histogram with Normal Curve.

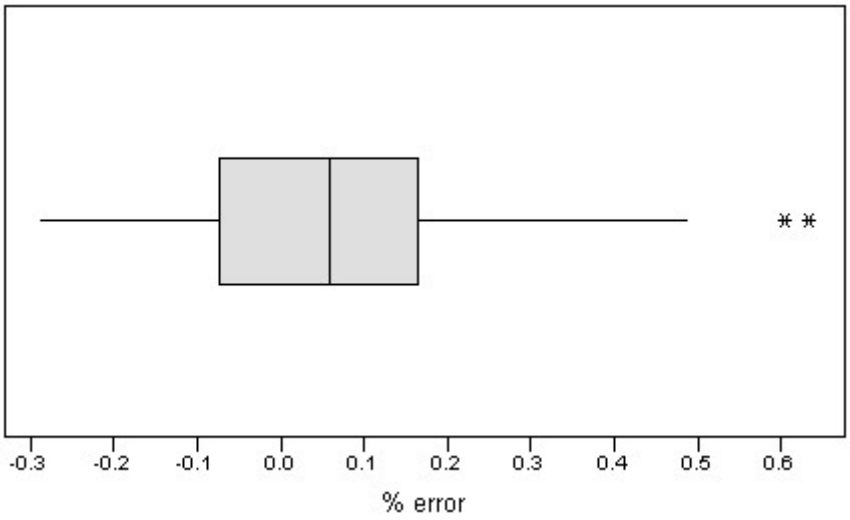


Figure 49A. Percent Error Box Plot.

# LIST OF REFERENCES


[1] H. I. H. Saravanamuttoo, H. Cohen, C. F. C. Rogers, *Gas Turbine Theory*. Longman Group Limited, 1972.

[2] H. I. H. Saravanamuttoo, S. A. Sjolander, J. E. D. Gauthier, P. V. Straznicky, *Gas Turbine Performance and Design.* Carleton University, 2002.

[3] United Technologies Corporation Publications Department. *Gas Turbine Engine and Its Operation.* United Technologies Pratt & Whitney Operating Instructions, 1988.

[4] Siemens-Westinghouse Compressor Design and Development Group. *Combustion Turbine Mechanical Design Criteria.* SWPC Technical Library, 2004.

[5] P. Garbett, T. Zagar, *Compressor FOD (Foreign Object Damage)Tolerance.* SWPC Library Technical Reports, 2000.

[6] R. Dorris (private communication), 2002.

[7] N. Davis, *Compressor Diaphragm LE and TE Stress Fields*. SWPC Library Technical Reports, 2001.

[8] G. Genta, E. Brusa, *Rotordynamic Analysis In The Design Of Rotating Machinery.* Mechanics Department, Politecnico di Torino, 1996.

[9] D. Hutton, *Applied Mechanical Vibrations.* McGraw-Hill Book Company, 1981.

[10] R. B. Heywood, *Designing Against Fatigue.* Chapman and Hall LTD, 1962.

[11] D. G. Wilson, *The Design of High-Efficiency Turbomachinery and Gas Turbines.* The MIT Press, 1984.

[12] M. Singh, T. Matthews, *Fatigue Damage of Steam Turbine Blade Caused by Frequency Shift Due to Solid Buildup.* Dresser-Rand Wellsville N.Y., USA, 1995.